CrossMark

Piecewise Trajectory Replanner for Highway Collision Avoidance Systems with Safe-Distance Based Threat Assessment Strategy and Nonlinear Model Predictive Control

Umar Zakir Abdul Hamid[1] · Mohd Hatta Mohammed Ariff[1] · Hairi Zamzuri[1] ·
Yuichi Saito[2] · Muhammad Aizzat Zakaria[3] · Mohd Azizi Abdul Rahman[1] ·
Pongsathorn Raksincharoensak[2]

Abstract This paper proposes an emergency Trajectory Replanner (TR) for collision avoidance (CA) which works based on a Safe-Distance Based Threat Assessment Strategy (SDTA). The contribution of this work is the design of a piecewise-kinematic based TR, where it replans the path by avoiding the invisible rectangular region created by SDTA. The TR performance is measured by assessing its ability to yield a maneuverable path for lane change and lane keeping navigations of the host vehicle. The reliability of the TR is evaluated in multi-scenario computational simulations. In addition, the TR is expected to provide a reliable replanned path during the increased nonlinearity of high-speed collisions. For this reason, Nonlinear Model Predictive Control (NMPC) is adopted into the design to track the replanned trajectory via an active front steering and braking actuations. For path tracking strategy, comparisons with benchmark controllers are done to analyze NMPC's reliability as multi-actuators nonlinear controller of the architecture to the CA performance in high-speed scenario. To reduce the complexity of the NMPC formulation, Move Blocking strategy is incorporated into the control design. Results show that the CA system performed well in emergency situations, where the vehicle successfully replanned the obstacle avoidance trajectory, produced dependable lane change and lane keeping navigations, and at the same time no side-collision with the obstacle's edges occurred. Moreover, the multi-actuators and nonlinear features of NMPC as the PT strategy gave a better tracking performance in high-speed CA scenario. Assimilation of Move Blocking strategy into NMPC formulation lessened the computational burden of NMPC. The system is proven to provide reliable replanned trajectories and preventing multi-scenario collision risks while maintaining the safe distance and time constraints.

Keywords Collision avoidance · High speed collision · Path planning · Nonlinear model · Model predictive control · Active safety

1 Introduction

The vehicle automation field has seen a lot of progress since 1970*s* [1]. Nevertheless, the number of road fatalities remains high globally. In Japan, collisions which involved moving obstacles show an escalated value since 2008 [2]. While in Malaysia, high speed collisions continue to be the most common types of road fatalities [3, 4]. The host vehicle is considered to be moving in a low speed if its current speed is in the range of $30 - 40 \, km/h$, medium speed for a car traveling up to $50 - 90 \, km/h$ and for high speed vehicle, the value is $100 \, km/h$ onwards [5–8]. Most of the road accidents occurred due to the driver inattentiveness and fatigue (human error) [9]. Owing to this, Advanced Driver Assistance Systems (ADAS) was introduced as part of the vehicle active safety feature [10]. One of the systems which fall under ADAS umbrella is collision avoidance (CA), which

✉ Hairi Zamzuri
hairi.kl@utm.my

1 Vehicle System Engineering iKohza, Malaysia-Japan International Institute of Technology, Universiti Teknologi Malaysia, 54100, Kuala Lumpur, Malaysia

2 Department of Mechanical Systems Engineering, Tokyo University of Agriculture & Technology, Nakacho 2-24-16, Koganei, Tokyo 184-8588, Japan

3 Faculty of Manufacturing Engineering, Universiti Malaysia Pahang, 26600 Pekan, Pahang, Malaysia

has been reported to reduce human error [11]. The inclusion of CA as an important safety feature for highway vehicles by the National Transportation Safety Board of the United States in their 2016 Report has turned CA into one of the progressing research areas in the aforementioned field [12].

Although there have been a lot of advances in the CA research, the current collision warning devices are not fully efficient in alerting the drivers in cases occurred due to the driver inattentiveness (e.g. avoidance which involve multi-lane maneuver) [13]. Furthermore, a lot of CA failures involve the host vehicle to collide with the obstacle's edge [14]. Besides that, in high-speed multi-lane highway scenario, a simple TR and PT strategies are insufficient for a dependable CA navigation. In the previous works of [2, 13] and [14], the controllers are designed for low and medium speed case studies. Thus, the efficiency of the system in high-speed contexts are not evaluated. There have been also reported near-miss incidents between the host vehicle and obstacle [15]. This is due to the failure of collision warning system to warn the driver to replan new path in appropriate time. Relying on these facts, it is a necessity for a CA system which considers all of the aforementioned issues.

A regular CA system usually consists of a complex combined architecture of Threat Assessment, Trajectory Replanning and Path Tracking strategies (Fig. 1). Among the examples can be found in [24–26] and [27]. TA provides an online evaluation of the potential threat to the vehicle. The risk assessment aids the control interventions' activation in emergency situations by providing thresholds for the trajectory replanning actions. Though there are many types of TAs, such as Time-To-Collision (TTC) [14, 28], Required Deceleration Method (RDM) [29] and Time-Headway (TH) [30, 31], these strategies do not express the risk of multi-scenario collisions. For example, TH does not consider the collision risk with the obstacle's exact physical dimension into its formulation [30]. Hence, a TA which is based on the online safe-distance constraints between the host vehicle and the whole obstacle's dimension (i.e. frontal vehicle)

is critically needed in the CA design architecture. This is important especially in the case of highway collision, where an unreliable TA might result to badly timed lane change behavior thus resulting side collision with the obstacle's edge.

In [32], an extensive review of motion planning for autonomous systems have been discussed. However, most of the strategies are not suitable for cars and car-like mobile robots due to their non-holonomic dynamic constraints [33]. One of the earliest path planning work that relates to car dynamics is reported in [34], where a particle's path with constrained curvature is analyzed and the shortest path which consists of features with minimal curvature is determined [35]. It is suggested that this strategy can be applied to cars and car-like robots, due to the constrained curvature which resulted from their non-holonomic and physical constraints [35]. However, such path planning methods only assessed the obstacle-free environments [35]. On the other hand, [14] has adopted a geometrical path planning based on the Time-To-Collision strategy. Although the CA system is capable of mitigating the crash, a slight collision with the obstacle's edge is inevitable. For high-speed avoidance of moving obstacles, a non-complex TR which considers the hazard of side collision should be considered to alleviate the computational process. Thus, for a reliable trajectory replanning, a geometrically and kinematically suitable replanned route must be determined to ensure a constant relative safe distance between the host vehicle and obstacle.

Path Tracking control of a CA system allows the vehicle to follow the replanned trajectory in an emergency situation [36]. A decent PT should provide multiple-input and multiple-output (MIMO) actuations to handle high non-linearity of high-speed collisions and moving obstacles scenarios, as well as possesses low computational time [37]. One of the well-known examples is Model Predictive Control (MPC). MPC is a control technique which originated from process engineering field and has widely been used

Fig. 1 Typical architecture of Vehicle Collision Avoidance systems
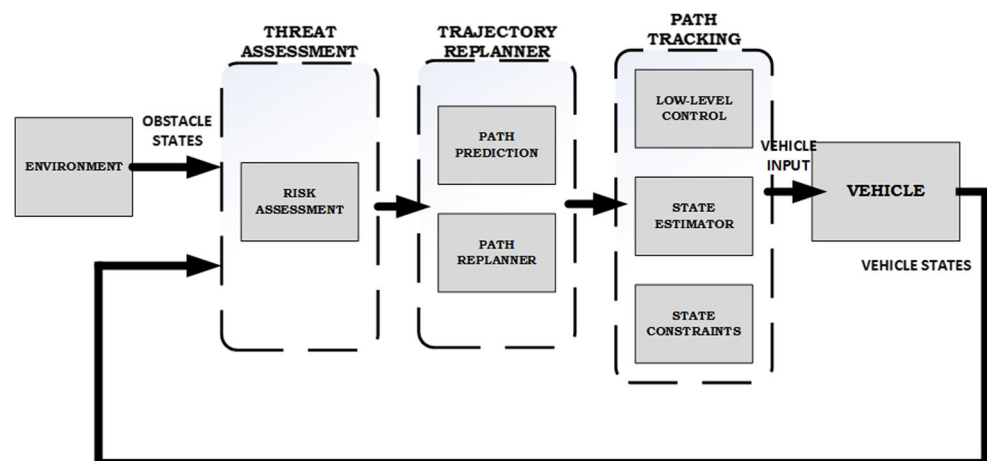
in the vehicle active safety applications recently [26, 38–40]. MPC utilizes the plant dynamics model to predict the system future states and optimizes the instantaneous process control performance at a defined time step [40]. With the capacity to consider the actuators' limitations (i.e. input constraints) for its control law formulations and swift online optimization, MPC technique offers attractive solutions for practical implementations [17, 41]. For high-speed collision scenarios, where the nonlinearity of the host vehicle dynamics is abruptly increased, a nonlinear PT is needed. In addition, to allow a feasible CA maneuver, MPC depends heavily on the model usage. Thus, a nonlinear vehicle model can be used for the control design and promises better vehicle dynamics for the said purpose. Therefore, the usage of Nonlinear MPC will be beneficial. However, the complexity of NMPC increases the computational time. This can be solved by assimilating computational burden minimizing strategy like Move Blocking Strategy [42].

Selection of right methods for TA, TR and PT will provide solutions to the common CA issues such as local minima (host vehicle oscillates continuously between obstacles) [43, 44], untimely controller actions [45] and risk of lane departure.

1.1 Outline and Contributions of the Paper

The main contribution of this paper is by introducing a TR design for a timely path replanning actions which aim to function in multi-scenario collision avoidance, as well as considers the vehicle nonlinearity and safe distance to the obstacles. This is achieved by introducing a comprehensive CA design with modular nature, where each of them works independently, enabling the strategies to be tuned and designed separately without affecting other blocks' performance. The side collision problem of previous works is hindered with the considerations of the full physical dimension of the obstacle into CA system formulation. This is done by providing an invisible rectangular safe region around the obstacle, which will prevent its collision with the host vehicle, regardless of the obstacle's size. To create maneuverable reference CA path, a simple piecewise-kinematic based trajectory replanning strategy is introduced. This strategy works in conjunction with the Safe-Distance Based Threat Assessment (SDTA). This ensures a feasible lane change and lane keeping maneuver during the CA maneuver. NMPC subsequently tracks the new replanned trajectory. This is done by determining appropriate vehicle steering angles and braking torques. NMPC is then compared to two benchmark controllers for analyses of its tracking performance. The first controller is Geometrical Based Method, which is a steering controller. The objective of the comparison is to see the effect of braking actuation absence from the system, especially at the high

speed. This is to justify the selection of NMPC as the MIMO controller. NMPC is also compared with another linear single-input and single-output (SISO) steering and braking torque controllers to study the importance of having nonlinear motion guidance controller in the system. To verify the efficiency of the design in providing reliable lane keeping and lane change behavior during hazards, it is evaluated in multi-objective collision avoidance scenarios. Besides that, to ensure that the system yields the path replanning action at the right time, its performance are evaluated against the time-to-collision between the host vehicle and the obstacles. The proposed design is expected to provide solutions to the aforementioned problems of untimely CA navigation, side collision, lane departure after CA maneuver and high-speed collision avoidance.

The paper is organized as follows. The next section describes the associated mathematical representations which include the kinematics and dynamics modeling of the host vehicle. In the following section, the proposed CA architecture is presented. Detailed formulations of SDTA and Piecewise-Kinematic based TR are written together with the NMPC control design. In the results section, the simulation outcomes are examined. Comparisons between NMPC and the benchmark controllers as the PT are discussed in the same section. Finally, the deduced conclusions and directions for future works are concisely written in the final sections.

2 Vehicle Model

This section consists of the mathematical modeling of the host vehicle dynamics and kinematics. The full model is a 4-wheeled vehicle, and the design and parameter are based on the previous work of the authors [2, 16]. The vehicle
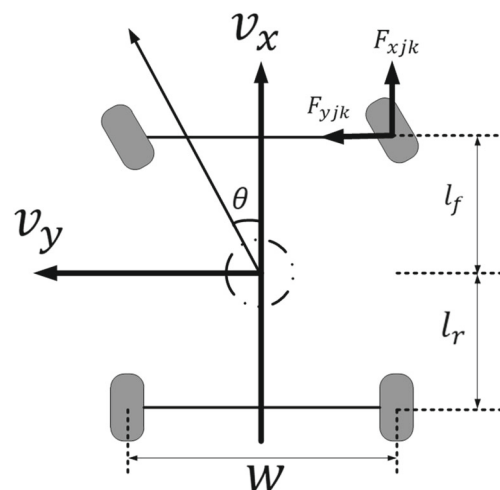

Fig. 2 3-DOF vehicle model used in this work

motion is represented by the dynamics model, while its whereabouts are represented by the kinematic models.

2.1 Vehicle Dynamics

The vehicle dynamics model is the relationship between the vehicle and the road surface, and it relies on the tire models [18]. The model has both steering and braking force inputs to the plant. It is a 3 degrees of freedom (3-DOF) vehicle as shown in Fig. 2. The proposed vehicle is incorporated with an active front steering. It depicts the vehicle's lateral and longitudinal motions as well as its yaw motion. The vehicle is assumed to navigate with a constant longitudinal velocity in a straight line. For brevity, the authors are neglecting the vehicle's initial acceleration.

The formulations for the vehicle dynamics are as denoted below:

$$\dot{v}_x = a_x + v_y \cdot r \tag{1}$$

$$\dot{v}_y = a_y - v_x \cdot r \tag{2}$$

$$F_{xfl} \cdot \cos \delta_F - F_{yfl} \cdot \sin \delta_F + F_{xfr} \cdot \cos \delta_F$$
$$- F_{yfr} \sin \delta_F + F_{xrl} + F_{xrr} = m_t \cdot a_x \tag{3}$$

$$F_{yfl} \cdot \cos \delta_F + F_{xfl} \cdot \sin \delta_F + F_{yfr} \cdot \cos \delta_F$$
$$+ F_{xfr} \sin \delta_F + F_{yrl} + F_{yrr} = m_t \cdot a_y \tag{4}$$

Equations 1 and 2 indicate the longitudinal and lateral vehicle accelerations, while Eqs. 3 and 4 represent the summations of the longitudinal and lateral forces, respectively. The host vehicle mass is symbolized by m_t. The tire forces which act relative to the vehicle body frame are denoted by F_{ijk}, where i represents the force direction (x, longitudinal and y, lateral) and jk represents the tire positions ($fl = front\ left, fr = front\ right, rl = rear\ left$ and $rr = rear\ right$). F_{ijk} relies on the vehicle kinematics model and f_{ijk}, the longitudinal and lateral forces which act along the tire axis [17]. The formulation for F_{ijk} is as below:

$$F_{xjk} = f_{xjk} \cdot \cos \delta_{jk} - f_{yjk} \cdot \sin \delta_{jk} \tag{5}$$

$$F_{yjk} = f_{xjk} \cdot \sin \delta_{jk} + f_{yjk} \cdot \cos \delta_{jk} \tag{6}$$

δ_{jk} in Eqs. 5–6 denotes the vehicle steering angle. δ_F and δ_R indicate the frontal and rear steering angles, respectively. Since the host vehicle possesses an active front steering, δ_R is assumed to be constantly zero. Figure 3 depicts the working principle of δ_{jk}.

In Eqs. 1–4, r is the vehicle yaw rate where $\dot{r}$, the yaw motion is formulated as below:

$$\dot{r} = \frac{1}{J_z} \cdot (\frac{w}{2}(F_{xfl} \cdot \cos \delta_F + F_{xfr} \cdot \cos \delta_F + F_{xrl} - F_{xrr})$$
$$+ (\frac{w}{2}(F_{yfl} \cdot \sin \delta_F - F_{yfr} \cdot \sin \delta_F) - l_r(F_{yrl} - F_{yrr})$$
$$+ l_f \cdot (F_{yfl} \cdot \cos \delta_F + F_{yfr} \cdot \cos \delta_F - F_{xfl} \cdot \sin \delta_F - F_{xfr} \cdot \sin \delta_F)) \tag{7}$$
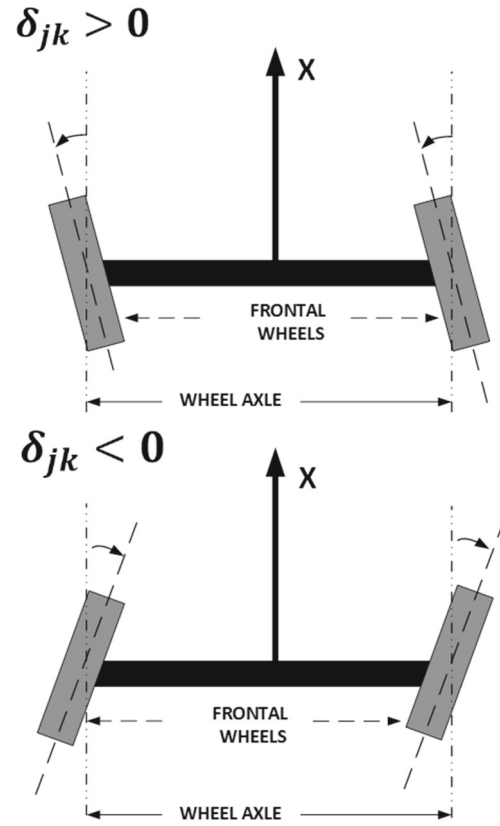
Fig. 3 Illustration of steering angle working principal. The vehicle will navigate to the left side if δ_{jk} is larger than $'0'$ and to the right side if it is less than $'0'$

where J_z depicts the vehicle yaw inertia, while l_f and l_r each represents the length from the vehicle center of gravity (COG) to the front and rear tracks respectively. w in Eq. 7 denotes the vehicle track width. Equations 1–7 is adopted from the work of [19], where it is a standard representation of vehicle dynamics. For this work, the road frictions are assumed to be of constant value.

2.2 Tire and Braking Model

There are many approaches for the tire modeling. These include the Fiala tire model, which is utilized due to its simplicity and little usage of parameters [18], Lacombe tire model, which is based on mechanical analogies [20], Flexible Structure Tire Model (FTire), a model which is derived from the structural dynamics approach [21], Dugoff tire model as well as Pacejka's Magic Formula — perhaps the most well-known tire model which was derived from experimental data [22]. For this work, Pacejka's Magic Formula are utilized for the lateral tire forces formulation due to its simplicity and ability to provide optimal tire characteristics

[16]. The forces which act along the tire lateral axis, f_{yjk} are:

$$f_{yjk} = \sqrt{(\mu_{jk} F_{zjk})^2 - f_{xjk}^2} \cdot \sin(C_{jk} \arctan(B_{jk} \alpha_{jk})) \quad (8)$$

where F_{zjk} represents the normal force of each tires, μ_{jk} denotes the friction coefficient and C_{jk} as well as B_{jk} respectively indicate the tires parameter [46]. As Pacejka Magic Formula requires the host vehicle lateral tire slip angles as input for its calculations, the formulations for the tire slip angles are denoted below:

$$\alpha_{fl} = \delta_F - \arctan(\frac{U + l_f \cdot r}{V}) \quad (9)$$

$$\alpha_{fr} = \delta_F - \arctan(\frac{U + l_f \cdot r}{V}) \quad (10)$$

$$\alpha_{rl} = \delta_R + \arctan(\frac{l_r \cdot r - U}{V}) \quad (11)$$

$$\alpha_{rr} = \delta_R + \arctan(\frac{l_r \cdot r - U}{V}) \quad (12)$$

α_{jk}, the tire slip angle is formulated based on the U and V, the lateral and longitudinal velocities, respectively as well as its yaw rate and steering angle [16].

The combination of both longitudinal and lateral motion controls (i.e. steering and braking actuations) permits a more dependable CA navigation [14]. There are many ways to best distribute the braking forces, for example, the pro-and-contra cornering method [47], but for briefness, this paper deploys a simple braking forces distribution, adopted from the works of [24] as the aim is for the braking actuator to provide vehicle deceleration on an intact road surface. Thus, the proposed distribution is sufficient. For future work involving more complicated road scenarios which consider varying road frictions, a more complex torque distribution will be adopted.

The braking forces, F_B are distributed as the forces which act along the tire longitudinal axis. The formulations are:

$$f_{xfl} = f_{xfr} = D \cdot \frac{F_B}{2} \quad (13)$$

$$f_{xrl} = f_{xrr} = (1 - D) \cdot \frac{F_B}{2} \quad (14)$$

Equations 13 and 14 are illustrated in details in Fig. 4. D is the ratio of braking distributions, and in this work, the ratio of braking force distribution to the vehicle frontal part is higher than the rear part since the vehicle frontal wheel load is bigger due to the engine placement in the vehicle's front.

2.3 Vehicle Kinematics

Kinematics model refers to the vehicle current whereabouts and its coordinate in a certain instant. It is the geometric features of the vehicle motion and is described in relation to the inertial and ground-fixed frame [48]. In this work, the
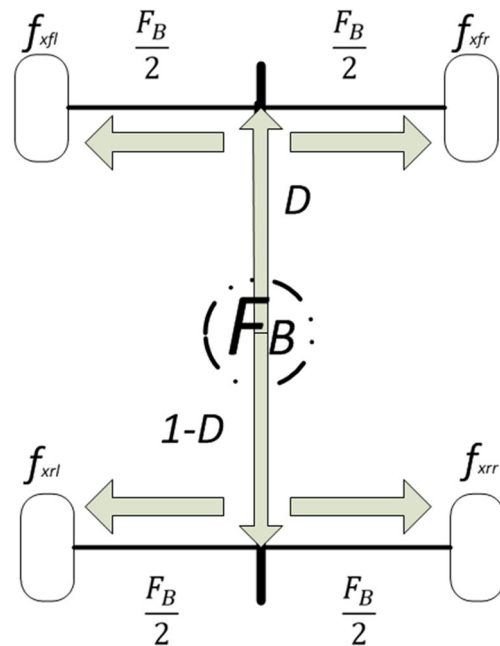

Fig. 4 Braking Force Distribution

vehicle current and future whereabouts are projected along the road centerline, relative to the obstacle positions as well as in respect to its inertial frame.

The vehicle general motion; its position and orientation are described by the following:

$$\eta_{position} = (x_{cur} \; y_{cur})^T \quad (15)$$

$$\eta_{orientation} = (\theta_{cur} \; \dot{\theta}_{cur})^T \quad (16)$$

η describes the position and orientation of the vehicle where the vehicle is moving in a (x_{cur}, y_{cur}) coordinate with orientation, θ_{cur}. The full vehicle kinematics model equations are jotted down below:

$$\dot{x}_{cur} = V \quad (17)$$

$$\dot{y}_{cur} = U \quad (18)$$

$$\dot{\theta}_{cur} = r \quad (19)$$

$$\rho = \frac{1}{R} \quad (20)$$

V and U are formulated as:

$$V = (\frac{R}{R - y_{cur}}) \cdot (v_x \cdot \cos \theta_{cur} - v_y \cdot \sin \theta_{cur}) \quad (21)$$

$$U = v_y \cdot \cos \theta_{cur} + v_x \cdot \sin \theta_{cur} \quad (22)$$

where R denotes the curvature radius and ρ is the road curvature. Formulations 17–22 are adopted from [49]. It is important to mention that the vehicle is assumed to move initially in a straight line, neglecting curvilinear trajectory.
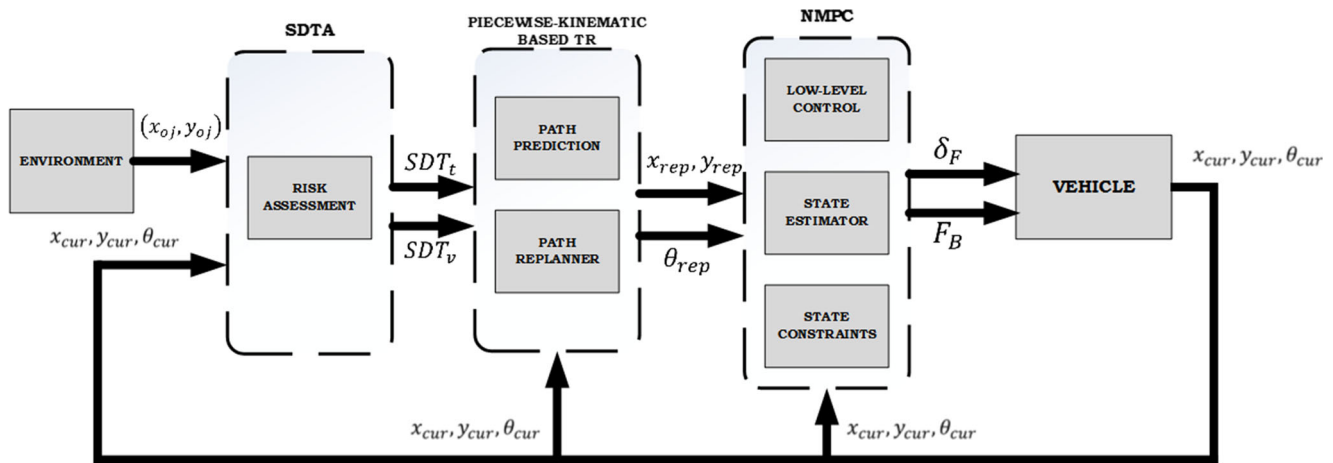
Fig. 5 Proposed Architecture of the work

3 Vehicle Collision Avoidance System Architecture Design

In this section, the authors discuss the proposed CA architecture (Fig. 5). The formulations for each of the strategies are written in their respective subsections. The TR overrides the current host vehicle trajectory with a new replanned path when the SDTA threshold is violated. NMPC acts as the Path Tracking to guide the vehicle motion during the emergency states.

3.1 Safe-Distance Based Threat Assessment Strategy

Several strategies have been used to measure the metrics of potential collisions. Among notable examples of TA are Time-to-X [50, 51], Probabilistic Method [52] as well as Artificial Potential Field [2, 13]. However, the drawbacks are they do not measure the obstacle's full physical dimensions into calculations, thus increasing the risk of the side collision, despite some of them having simple computations [50]. In addition, there have been reported the cases of local

minima with the Potential Field, where the host vehicle oscillates infinitely between the obstacles [14].

In this paper, the authors opted to use a safe distance based strategy (SDTA) as the TA for the CA design. The output from the SDTA is utilized for the decision-making strategy of the emergency trajectory replanner as well as the braking force distribution states. The strategy provides an online distance calculation from the host vehicle to the obstacle. SDTA is formulated based on the works of [49] and [55]. Compared to the previous works, this paper integrates the SDTA with a piecewise-kinematic trajectory replanner for the path replanning. In addition, TR formulation allows it to yield a feasible replanned path in the high-speed collision, which is not considered in the previous works. SDTA calculates the safe distance between each host vehicle's edges to the obstacle's Center of Gravity (COG). Based on the distances from each edge, a rectangular safe region is created around the obstacle. The main idea is to create a safe region around the obstacle, despite its physical measurement, ensuring a constant safe distance which the host vehicle will avoid (Fig. 6). SDTA assists the host vehicle

Fig. 6 Online calculation of SDTA while host vehicle avoiding the obstacle, ensuring a constant safe distance from potential hazard
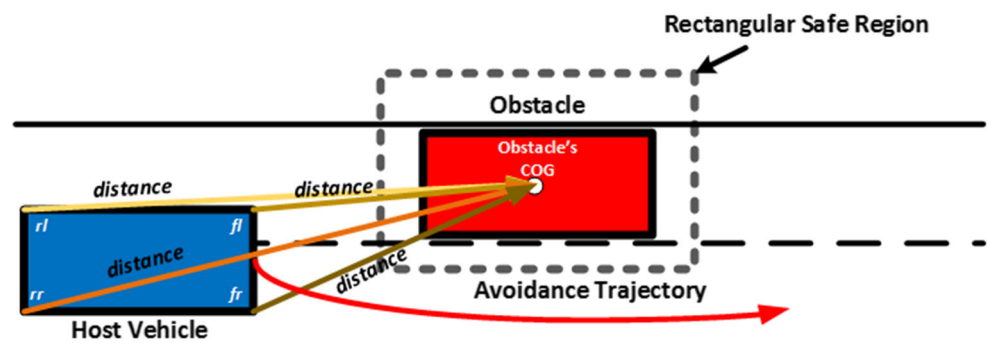
in maintaining a safe distance from the frontal obstacle. Once the threshold, SDT_t is violated, TR replans the current trajectory to an avoidance trajectory based on the current SDTA values, SDT_v. In this section, the SDTA formulation is jotted down.

3.1.1 Obstacle Dimensions

In the year 2011, it is reported that the majority (57.7 %) of the marketed vehicle in the European Union consists of the A, B and C-Segment vehicles (European Commission Standard), which has the maximum length of 4.4 m [53, 54]. Based on this finding, in this work, the frontal obstacles are assumed to be of the said length dimensions.

3.1.2 Safe Distance Formulation

$$\dot{d}_{xoj} = V_{oj} - V \tag{23}$$
$$\dot{d}_{yoj} = U_{oj} - U \tag{24}$$

In Eqs. 23–24, the vehicle's motion in relation to the obstacles are written. d_{xoj} and d_{yoj} are the longitudinal and lateral distances between the vehicle and the obstacle's COG, while the obstacle's longitudinal and lateral velocities are denoted by V_{oj} and U_{oj}. To ensure a more precise safe distance, the distances from each of the vehicle edges to the obstacle's COG are calculated. The calculations are based on the vehicle's (x_{cur}, y_{cur}), relative to the obstacle.

$$\begin{bmatrix} d_{xoj,fl} \\ d_{yoj,fl} \end{bmatrix} = \begin{bmatrix} d_{xoj} \\ d_{yoj} \end{bmatrix} + \begin{bmatrix} \cos\theta_{cur} & -\sin\theta_{cur} \\ \sin\theta_{cur} & \cos\theta_{cur} \end{bmatrix} \begin{bmatrix} -l_f \\ -\frac{w}{2} \end{bmatrix} \tag{25}$$

$$\begin{bmatrix} d_{xoj,fr} \\ d_{yoj,fr} \end{bmatrix} = \begin{bmatrix} d_{xoj} \\ d_{yoj} \end{bmatrix} + \begin{bmatrix} \cos\theta_{cur} & -\sin\theta_{cur} \\ \sin\theta_{cur} & \cos\theta_{cur} \end{bmatrix} \begin{bmatrix} -l_f \\ \frac{w}{2} \end{bmatrix} \tag{26}$$

$$\begin{bmatrix} d_{xoj,rl} \\ d_{yoj,rl} \end{bmatrix} = \begin{bmatrix} d_{xoj} \\ d_{yoj} \end{bmatrix} + \begin{bmatrix} \cos\theta_{cur} & -\sin\theta_{cur} \\ \sin\theta_{cur} & \cos\theta_{cur} \end{bmatrix} \begin{bmatrix} l_r \\ -\frac{w}{2} \end{bmatrix} \tag{27}$$

$$\begin{bmatrix} d_{xoj,rr} \\ d_{yoj,rr} \end{bmatrix} = \begin{bmatrix} d_{xoj} \\ d_{yoj} \end{bmatrix} + \begin{bmatrix} \cos\theta_{cur} & -\sin\theta_{cur} \\ \sin\theta_{cur} & \cos\theta_{cur} \end{bmatrix} \begin{bmatrix} l_r \\ \frac{w}{2} \end{bmatrix} \tag{28}$$

The lateral and longitudinal distances from each of vehicle's edges to the obstacle's COG (obtained from Eqs. 25–28) is then divided with the obstacle's (frontal vehicle) length and width to normalize the vectors. Using the infinity norm (max function), a rectangular safe region (vector norm) is obtained from the normalized vector. The infinity norm outputs a value, SDT_v that is larger than SDT threshold, SDT_t, ensuring a constant rectangular safe region regardless the obstacle's dimension [49, 55]. Although this work only considers the frontal vehicles of the size of C-Segment and smaller class, for the collision scenarios with multi-size frontal vehicle, SDTA will remain functional by having larger threshold defined for the larger obstacle.

The current value of SDT_v at an instant is expressed as below:

$$\left\| \begin{bmatrix} \dfrac{2 \cdot d_{xoj,jk}}{l_{oj}} \\ \dfrac{2 \cdot d_{yoj,jk}}{w_{oj}} \end{bmatrix} \right\|_\infty = \left\| d_{oj,jk} \right\|_\infty \tag{29}$$

$$SDT_v = \left\| d_{oj,jk} \right\|_\infty \tag{30}$$

$$\left\| SDT_v \right\|_\infty \geq SDT_t \tag{31}$$

In Eq. 31, by having the distances from each of vehicle's edges to the obstacle's COG normalized, the infinity norm created a safe rectangular region consists of SDT_v from each edge. To ensure a constant safe distance between the vehicle to the obstacle, a threshold, SDT_t, is given and must not be violated. To accommodate the vehicle dynamics constraint, SDT_t should be high enough to enable a feasible vehicle movement, especially in higher speed. TR then replans the path to avoid this rectangle. SDT_v will be the base of the decision making for the trajectory replanning and the braking force distribution states. Equations 23–31 are based on the works of [49] and [55].

Figure 7 illustrates the top view depiction of Eqs. 25–28, where the distance from each of vehicle's edges to the obstacle's COG is calculated. Meanwhile, Fig. 8 depicts the rectangular safe region that is obtained when Eqs. 29–31 are
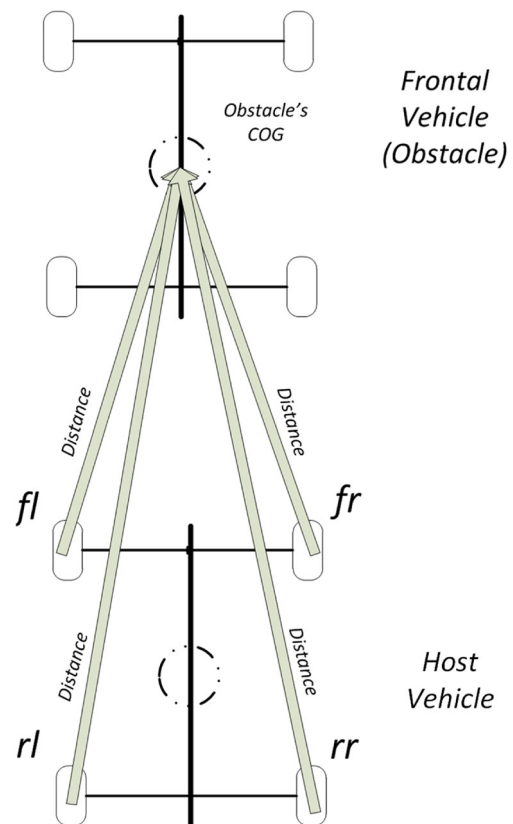

Fig. 7 Top view illustration of SDTA Formulation
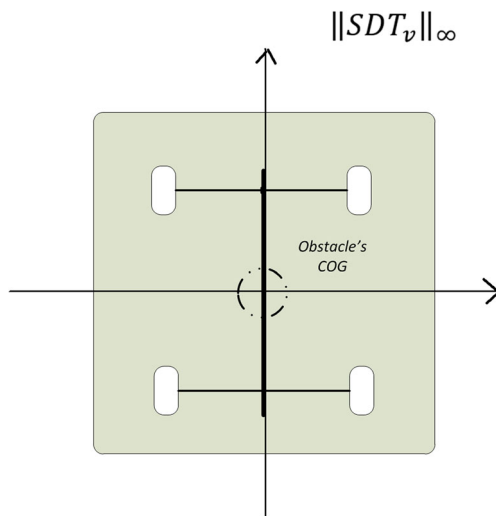
$$\|SDT_v\|_\infty$$

Obstacle's
COG

Fig. 8 Rectangular safe region provides a constant safe distance threshold to be avoided by the host vehicle

calculated. The formulation of SDTA is done online, so the distance from each corner of the host vehicle to the obstacle's COG is done at each instant. Thus, a constant safe distance is ensured (Fig. 6).

Although this is a simulation-based work, it is important to briefly mention the real-time implementation's requirement of the algorithm for future references. The obstacle dimension which is required for the implementation of SDTA can be feasibly obtained by utilizing the radar sensors, which will locate the (x, y) coordinate of the obstacle's COG. To ensure the threat assessment is robust enough regardless of the vehicle dimensions in real-time, an extensive vehicle classification study of certain demographics

is required in the future to be integrated with the algorithm. This will allow the rectangular region to fit all types of the vehicle of all dimensions and consequently become practical to be used with a fully autonomous vehicle.

3.1.3 Time-to-Collision Verification

To analyze the efficiency of the SDTA as threat assessment, a calculation of the time-to-collision between x_{cur} to the obstacle's current x-axes coordinate in each scenario is formulated based on the formulation below,

$$TTC = ||\frac{x_{or} - x_{cur}}{v}|| \tag{32}$$

where x_{or} is the obstacle's rear x coordinate in relation to the current host vehicle x position, x_{cur} and v, velocity.

3.2 Piecewise-Kinematic Based Trajectory Replanner

In this section, the trajectory replanning (TR) computation is discussed. Among common problems of Path Planning are the complicated calculations as well as incidents of local minima and the negligence of vehicle non-holonomic constraints [57–59]. However, for high-speed collision avoidance, a simple TR is needed to allow the fast response of the system in the emergency scenario. As real drivers usually consider the risk of lane departure and the frontal vehicle in the occasion of multi-lane highway collisions [13], thus for the replanning action, these two factors will be incorporated into the calculation.

The trajectory replanning strategy which is proposed by the authors are based on the vehicle kinematics model and its decision making is based on the SDTA block.

Fig. 9 Host vehicle (x, y) coordinates; where during the avoidance, the kinematics are symbolized as x_{rep}, y_{rep}, while during no obstacle emergence, the coordinates are formulated as x_{cur}, y_{cur}
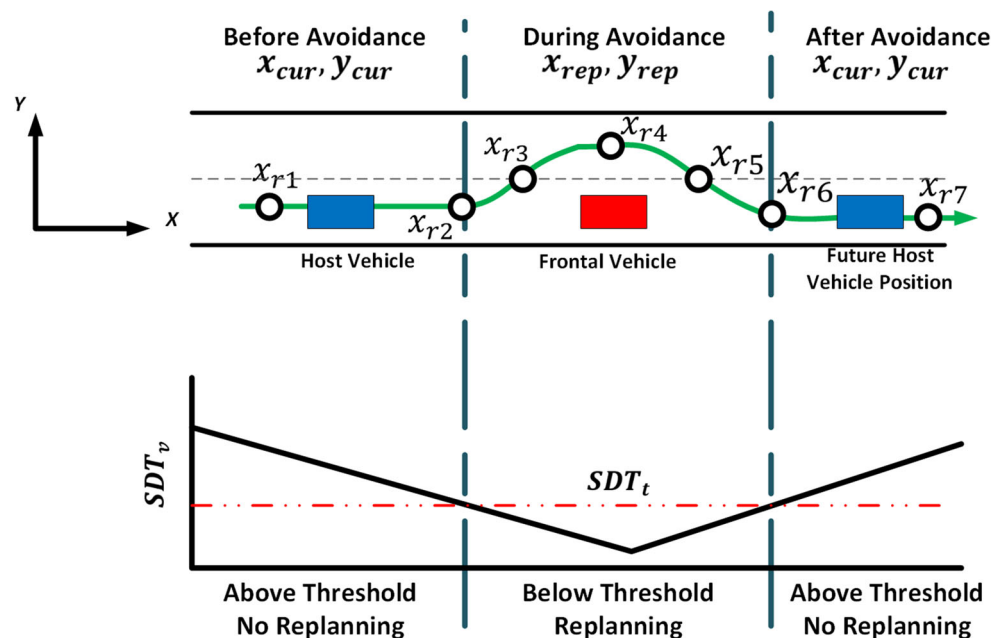
The piecewise-kinematic based TR discretely changes the vehicle kinematic orientation (heading) according to the current SDT_v and SDT_t. The reference replanned trajectory according to the SDTA outputs is illustrated in Fig. 9.

3.2.1 Vehicle Kinematics during Collision Avoidance

The emergency replanned trajectory is divided into seven zones, $x_{r1} - x_{r7}$ (Fig. 9). All of this zones are based on the current SDT_v. The desired path is obtained by having an adaptive varying vehicle heading, which is related to the SDT_v. The desired replanned vehicle coordinates, (x_{rep}, y_{rep}) is formulated as below, where the new trajectory is obtained by changing the host vehicle's heading at each zone:

$$x_{rep} = (\frac{R}{R - y_{cur}}) \cdot (v_x \cdot \cos\theta_{rep} - v_y \cdot \sin\theta_{rep}) \quad (33)$$

$$y_{rep} = v_y \cdot \cos\theta_{rep} + v_x \cdot \sin\theta_{rep} \quad (34)$$

To make a left turn, the vehicle heading (in accordance to the current road lane) is increased to a positive angle, while for a right turn, it is decreased to a negative angle. This in return creates a sinusoidal-alike reference trajectory. The advantage is that it depends on the SDT_v, where the vehicle will continue to navigate on the replanned trajectory if it is not safe to return to the original path. Only after the SDT_v is large enough the trajectory replanning computation ends. The generality of the formulation allows for multi-scenario CA navigation. The terminal vehicle's heading angle from the road centerline during the path replanning should be $'0'$. The integration of the SDTA into the TR ensures a precise and timely path replanning action. The division of the reference replanned trajectory into many zones assures a piecewise based TR action which accommodates the vehicle dynamics and considers its kinematics.

3.2.2 Reference Replanned Trajectory Formulation

The decision making strategy for the TR is written in this subsection. As real vehicle collisions might occur in various scenarios, the proposed piecewise-kinematic based TR must be able to provide feasible avoidance trajectory regardless of the risk situations.

The reference replanned trajectory is designed to accommodate the road vehicle and car-like robots' non-holonomic features. It is discretized into several zones, where each zones refer to the vehicle position in relation to its SDT_v (Fig. 9). For example, when the vehicle is at x_{r1}, its current SDT_v are larger than SDT_t. Piecewise function below denotes $x_{r1} - x_{r7}$ in more details. It considers SDT_v, SDT_t

as well as the vehicle and obstacle's current longitudinal position into the formulations.

$$x_{cur} = \begin{cases} x_{r1} & \text{if } SDT_v > SDT_t \text{ and } x_{oj} > x_{cur} \\ x_{r2} & \text{if } SDT_v = SDT_t \text{ and } x_{oj} > x_{cur} \\ x_{r3} & \text{if } SDT_v = \frac{SDT_t}{2} \text{ and } x_{oj} > x_{cur} \\ x_{r4} & \text{if } SDT_v < SDT_t \text{ and } x_{oj} = x_{cur} \\ x_{r5} & \text{if } SDT_v = \frac{SDT_t}{2} \text{ and } x_{oj} < x_{cur} \\ x_{r6} & \text{if } SDT_v = SDT_t \text{ and } x_{oj} < x_{cur} \\ x_{r7} & \text{if } SDT_v > SDT_t \text{ and } x_{oj} < x_{cur} \end{cases} \quad (35)$$

x_{cur} denotes the current x coordinate of the host vehicle. The TR action will be activated in x_{r2}, once the SDT_v has reached the SDT_t. In x_{r6}, once the replanning action has been completed, the vehicle will return to its original trajectory in x_{r7}. Figure 9 depicts the TR formulation in relation to the Safe Distance Threshold. The SDTt are defined to comply with the vehicle stopping distance, to ensure a smooth collision avoidance [60].

As the TR action is done by changing the vehicle heading, θ_{cur} in relation to the current SDT_v, the piecewise function for the decision making strategy of the TR is:

$$\theta_{rep} = \begin{cases} \theta_{cur} & \text{if } x_{cur} = x_{r1} \\ \theta_{cur} + \theta_{pos} & \text{if } x_{cur} = x_{r2} \\ \theta_{cur} + \theta_{pos} & \text{if } x_{cur} = x_{r3} \\ 0 & \text{if } x_{cur} = x_{r4} \\ \theta_{cur} + \theta_{neg} & \text{if } x_{cur} = x_{r5} \\ \theta_{cur} + \theta_{neg} & \text{if } x_{cur} = x_{r6} \\ \theta_{cur} & \text{if } x_{cur} = x_{r7} \end{cases} \quad (36)$$

From the formulation above, θ_{cur} will be changed once the obstacle is detected. When the vehicle is located at x_{r2}, which means the SDT_t has been violated, θ_{rep}, the vehicle heading during the TR will be increased to enable a left turn for the vehicle. θ_{rep} will keep increasing gradually until the vehicle reached x_{r4}, where θ_{rep} will be $'0'$ before it gradually decreases for a right turn from $x_{r5} - x_{r6}$. After successfully avoiding the obstacle at x_{r7}, θ_{rep} from the road centerline will be θ_{cur} again (original heading). The vehicle heading changes relatively to the SDT_v. θ_{pos} and θ_{neg} in Eq. 36 represents the increased and decreased vehicle heading, respectively.

This formulation of TR action can be used for multi-scenario CA: static, multiple-static as well as dynamic (moving) obstacles. However, for the dynamic obstacle, several considerations are needed to ensure a replanned trajectory that accommodates the vehicle dynamics constraints.

3.2.3 Trajectory Replanning for Dynamic Obstacle

As CA with moving obstacles can be classified as CA in unknown environments, a real-time update between the vehicle's position and obstacle's whereabouts must

be obtained. Equations 23–24 calculates the difference between both the host vehicle and obstacle's velocities to get their relative distance. The difference between static and dynamic CA action is in the replanning metrics. As the vehicle is avoiding the collision with a moving obstacle, there is a need for a prolonged avoidance navigation. Thus, the CA path will be replanned with a larger lateral distance, y_{rep}. This is to aid the vehicle dynamics constraint, particularly in the high-speed highway collision avoidance. In Fig. 10, it is shown that the SDT_v graph for Dynamic CA are different since the obstacle is moving.

3.2.4 Braking Force Distribution States

NMPC yields two control inputs, steering angle and braking forces. The braking forces piecewise distribution formulation is as below:

$$F_B = \begin{cases} 0 & \text{if } x_{cur} = x_{r1} \\ F_B & \text{if } x_{cur} = x_{r2,r3,r4,r5,r6} \\ 0 & \text{if } x_{cur} = x_{r7} \end{cases} \qquad (37)$$

With this logic, F_B will be distributed according to the Eqs. 13–14. The braking force distribution states based on the SDTA will ensure the vehicle to move smoothly without unnecessary braking actuations. The braking force actuation inclusions into the CA is important, especially in the case of high-speed CA to prevent the vehicle from sliding away too far from the original track.

3.3 Nonlinear Model Predictive Control Path Tracking

In this section, the control design of NMPC as the path tracking strategy of the system is stated.

A multi actuators vehicle model is adopted and used in the control design. Due to the model nonlinearity, a nonlinear MPC is adopted. Once the reference replanned trajectory is available, Nonlinear Model Predictive Control (NMPC) acts as an automated motion guidance which enables the

host vehicle to follow the new path. Since the system will be validated in multi-scenario CA simulations, which will include high speed CA, this will result in a coupled highly nonlinear longitudinal and lateral vehicle dynamics during the CA navigation. Thus, the MIMO feature of NMPC enables it to act as an integrated low-level controller. NMPC provides appropriate actuators interventions, i.e. steering angle and braking torques during the avoidance.

NMPC predicts the future behavior and output of the vehicle model at each time step. This is done by predicting the model behavior in a finite given horizon. With the knowledge, it calculates the input to the controller in a certain prediction horizon [69]. The future states will then be utilized to minimize the NMPC cost function, which will provide the constrained finite time optimal input sequence, u^* to the vehicle model (steering angle and braking forces) at each sampling time instant. Only the first element of the calculated control variable sequence will be applied, and the others will be excluded. The NMPC formulation will then be formulated again at each of the subsequent instants, to acquire a new sequence of control inputs and states [38].

3.3.1 Nonlinear Model Predictive Control Design

The overall vehicle model and its states can be written briefly as:

$$\dot{\xi} = f(\xi(t), u(t)) \qquad (38)$$

where ξ is the vehicle states vector, $[U, V, \theta_{cur}, r, y_{cur}, a_x]^T$ and $u(t)$ is the input to the model, $[\delta_F, F_B]^T$. A right selection of the vehicle states is important to enable a successful MPC operation and prevents a too aggressive controller and control initial overshoot. In addition, it will allow an adequate trade-off between the variables in the optimization process [26].

An essential aspect in MPC calculation is its optimization formulation. In [24] and [49], MPC is used as a complementary to the driver model to prevent the violations of the

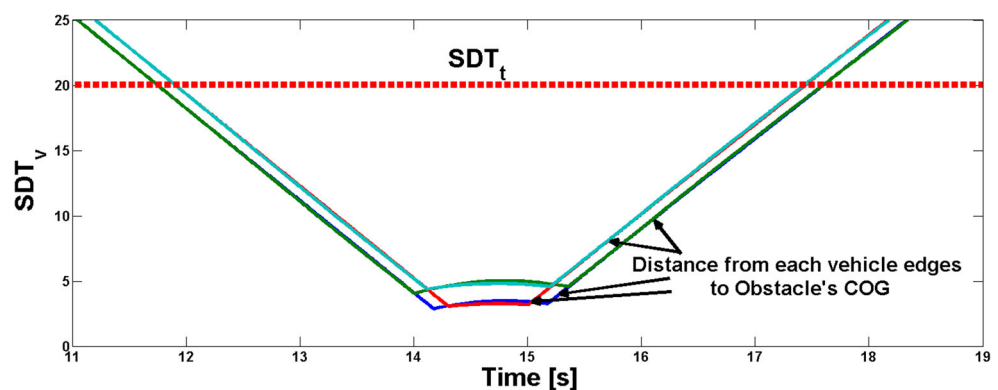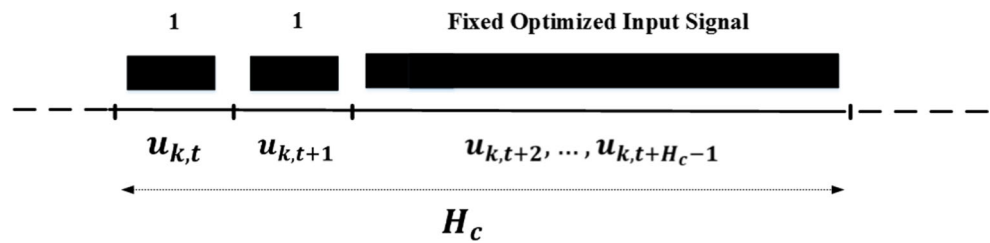**Fig. 10** SDT_v and SDT_t for Dynamic CA

Fig. 11 An example of move blocking implementation, where it fixes an optimized input signal for a certain period

safety constraints. However, in this work, NMPC is utilized as a trajectory tracking controller. The authors discretized with a fixed sampling time, T_s the overall system in Eq. 38 as below:

$$\xi_{k+1} = f^d(\xi_k, u_k) \tag{39}$$

The NMPC optimization cost is calculated as:

$$arg \min_{U_t} J_N(\hat{\xi}_k, u_k, \Delta u_k) \tag{40}$$

$s.t.$

$$\xi_{k+1,t} = f(\xi_{k,t}, u_{k,t}), \ k = t, \ldots, t + H_p - 1 \tag{41}$$

$$\Delta u_{k+1,t} = u_{k+1,t} - u_{k,t}, \ k = t, \ldots, t + H_c - 1 \tag{42}$$

$$u_{k,t} \in u, \ k = t, \ldots, t + H_c - 1 \tag{43}$$

$$\Delta u_{k,t} \in \Delta u, \ k = t + 1, \ldots, t + H_c - 1 \tag{44}$$

$$\xi_{t,t} = \xi_t \tag{45}$$

where t depicts the current instant and $\xi_{k,t}$ represents the future state vector at instant k, which is acquired by applying the optimal control sequence $u = [u_{t,t}, \ldots, u_{k,t}]$ to the vehicle overall system with $\xi_{t,t} = \xi_t$, the initial time. Meanwhile, $\Delta u_{k,t}$ is the control rate at k instant. It is the difference between the current control input value, $u_{k,t}$ to the value of previous instant, $u_{k,t-1}$. Only the first input vectors of the control horizon, H_c will be considered and taken as the optimization variables and H_p denotes the states

prediction horizon. For the cost function which the NMPC will minimize, the formulation is:

$$J_N(\xi_k, u_k, \Delta u_k) = \sum_{k=t}^{t+H_p-1} \left\| \xi_{k,t} - \xi_{ref} \right\|_G^2 + \left\| u_{k,t} \right\|_H^2$$
$$\left\| \ + \Delta u_{k,t} \right\|_I^2 \tag{46}$$

where ξ_{ref} is the reference replanned trajectory states and the first term of the cost function in Eq. 46 calculates the sum of tracking state deviations while the inputs are denoted by the second term and its input rate deviations, Δu by the third term. G, H and I respectively represents the weighting matrices of appropriate dimensions. G helps the first term in penalizing any deviations from the reference trajectory while H works to help the second term in preventing any sudden control increment. The weight matrices selections are important as improper weight choice will affect the vehicle current outputs and may suggest the vehicle to be understeered or oversteered [26].

For the closed-loop control law, the vehicle input is calculated from the optimized input trajectory, u_k in Eq. 39:

$$u_{k,t} = u_{k-1,t} - \Delta u_{k+1,t} \tag{47}$$

where for the next instance, the optimization iteration will be repeated and this continues until the end of the finite horizon [61]. For the NMPC design in this work, no lateral stabilization aspect is required since the adopted SDTA and TR already acted as the reference generator. The combination of the strategies is expected to keep the vehicle stability during high-speed maneuver and uncertainties.

Several constraints are included within the NMPC calculations, i.e. the constraints on the y_{cur}, α, δ_F as well as F_B.

Fig. 12 Geometrical Based Method Steering Controller (GMC) for comparison purpose
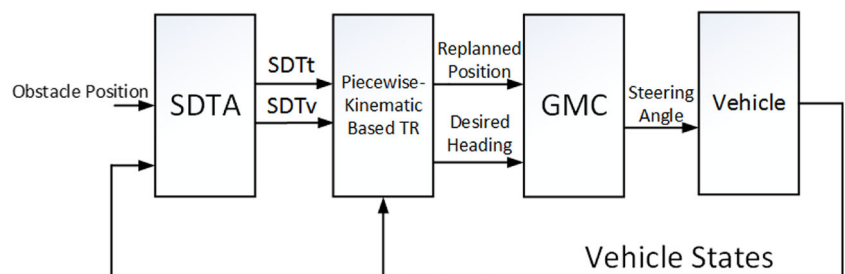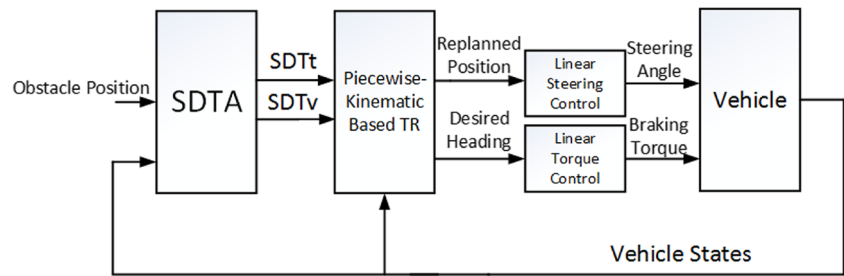
Fig. 13 Linear Steering and Torque Controllers for comparison purpose

This is to prevent sharp cornering and road departure during high-speed maneuver.

3.3.2 Move Blocking

The large extent of computational time required for the NMPC computation prevents it from becoming the favorable controller choice. However, there are many methods that can be used to reduce the NMPC calculation cost. Among them are the Move Blocking Strategy (MB) [62]. MB reduces the computational burden of an optimization process by fixing an optimized input signal for a longer control horizon. It parametrizes the manipulated variable trajectory and subsequently lessens the number of decision variables in an optimization. Among the examples of this strategy can be found in [63] and [64].

In this work, rather than utilizing the ordinary NMPC blocking (uniform blocking) [64], the authors incorporated the Move Blocking into the NMPC calculation, by constraining a set of neighboring manipulated variables (control input) to have an identical value. The parameters are shown in Table 2, where the blocks are set to be larger by the end of the finite horizon. The reason for this is due to the fact that input trajectory at the end of the horizon rarely gets applied. Thus, applying a larger block will save the calculation time and often sufficient [65]. In addition, since for NMPC, the nonlinearity of the model is maintained throughout the computation, this will help to reduce the computation loads.

For brevity, the formulation of Move Blocking used in this work is not written in details since it is adopted from the works of [63] and [65]. The suggested Move Blocking for the manipulated variable of the vehicle is [1 1 1 1 6] (Refer to Table 2). The constraints that are put into the last six control signal allow the computational complexity to be reduced. Figure 11 illustrated the concept of Move Blocking.

3.3.3 Benchmark Controllers

The proposed NMPC controller is then compared with two controllers. The first controller is a Geometrical-Based Method Steering Controller (GMC), derived from previous work in [66]. The comparison is done to analyze the performance of the same CA architecture when the braking force is present and while it is absent, due to the fact that GMC does not output braking forces from its calculation. In addition, the comparison is done to justify the needs of a multi-actuators controller as the Path Tracking strategy for high-speed CA. Figure 12 illustrates the CA architecture with GMC as the PT.

The second comparison is done to examine the advantage of NMPC as a nonlinear controller in high nonlinearity emergency situations (high-speed collisions). A comparison is done with Linear Steering and Torque controllers as the Path Tracking strategy. The control design is taken from our previous work in [2]. Compared to NMPC, the controllers are of the single-input and single-output (SISO) type. Figure 13 illustrates the CA architecture with linear steering and torque controllers as the PT.

Due to the modular nature of the architecture, the replacement of NMPC with both of the benchmark controllers is simply done. For conciseness, the performance analyses will be done with the collision scenario of moving obstacles only due to the aforementioned scenario having the highest nonlinearity. The analyses will involve comparisons of the vehicle avoidance trajectory during the hazard.

4 Simulations and Results

In this section, the simulation results for the CA architecture in Fig. 5 are written. The system is evaluated in a computational simulation using MATLAB. The host vehicle parameter are written in Table 1. Findings of each CA strategy blocks are discussed separately in their respective subsections to allow more detailed elaborations. In addition to that, the effects of Move Blocking strategy on the system

Table 1 Vehicle Parameter

Parameter	Symbol	Value
Mass	m_t	1529.98 kg
Width	w	1.55 m
Yaw Inertia	J_z	4000 kgm^2
COG length towards frontal part	l_f	1.14 m
COG length towards rear part	l_r	1.64 m

Table 2 Nonlinear Model Predictive Control Parameter

Symbol	Value
T_s	0.05(s)
H_p	21
H_c	10
Blocking	[1 1 1 1 6]
H	diag(0.3,0.003)
G	diag(0,0,40,1,11,1)
I	diag(0.3,0.003)
Constraint Softness	Hard

computation time is analyzed. The reliability of NMPC as the Path Tracking controller are compared with benchmark controllers.

4.1 Simulation Parameters

NMPC parameters are obtained using MPC Offline Tuning Method [67]. The tuning parameter selections are considered based on the objective function. This is to enable a well-balanced trade-off during the optimization between the variables. The wrong choice of states and weighting matrices will give significant impacts on NMPC motion guidance. H, G and I in Table 2 each indicates weighting matrices for the manipulated variables weight, manipulated outputs and the manipulated variables rate.

4.2 Simulation Descriptions

The objectives of the simulations are to verify the ability of the system to provide replanned trajectory in the occurrence of hazard while providing needed actuators' intervention for CA lane change and lane keeping actions. The authors decided to evaluate the architecture in four different scenarios on a straight road as the same approach can be easily extended to a winding road with a change of coordinates to a curvilinear reference frame. The descriptions of the proposed scenarios are discussed in their own subsections.

4.2.1 Scenario 1: Static Obstacle, Host Vehicle = 60 km/h

The vehicle moves on a straight road with an initial velocity of 60 km/h. The location of the frontal vehicle's (obstacle) COG is 330 m in front of the host vehicle initial position, (0, 0). As illustrated in Fig. 14a, the aim of this scenario is to see the architecture lane change and lane keeping performance for single static obstacle avoidance. The scenario is depicted based on the needs to avoid a priori unknown stranded vehicle in the case of highway traffic [3].

4.2.2 Scenario 2: Multiple Static Obstacle, Host Vehicle = 60 km/h

The vehicle moves on a straight road with an initial velocity of 60 km/h. The location of the first frontal vehicle is 330 m in front of the host vehicle initial position, (0, 0). The second obstacle is located at 500 m. The distance of the obstacles to each other is 170 m. As illustrated in Fig. 14b, the host vehicle will avoid the first obstacle before returning to its original trajectory. After the avoidance of the second obstacle, the host vehicle will not return to its original lane. Instead, it will continue to move in the new lane. The scenario usually happens in multi-lane highway collision where sometimes a return to the original lane is not possible due to the existence of other hindrance. The aim of this scenario is to see the architecture lane change and lane keeping ability during the proposed situation.
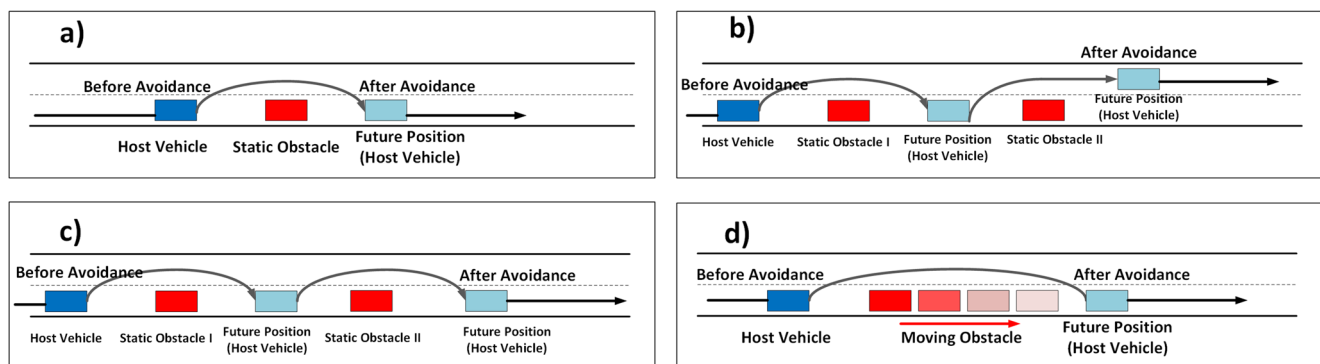

Fig. 14 Proposed Collision Avoidance Scenario, where (**a**), (**b**), (**c**) and (**d**) each represents the first, second, third and fourth scenario
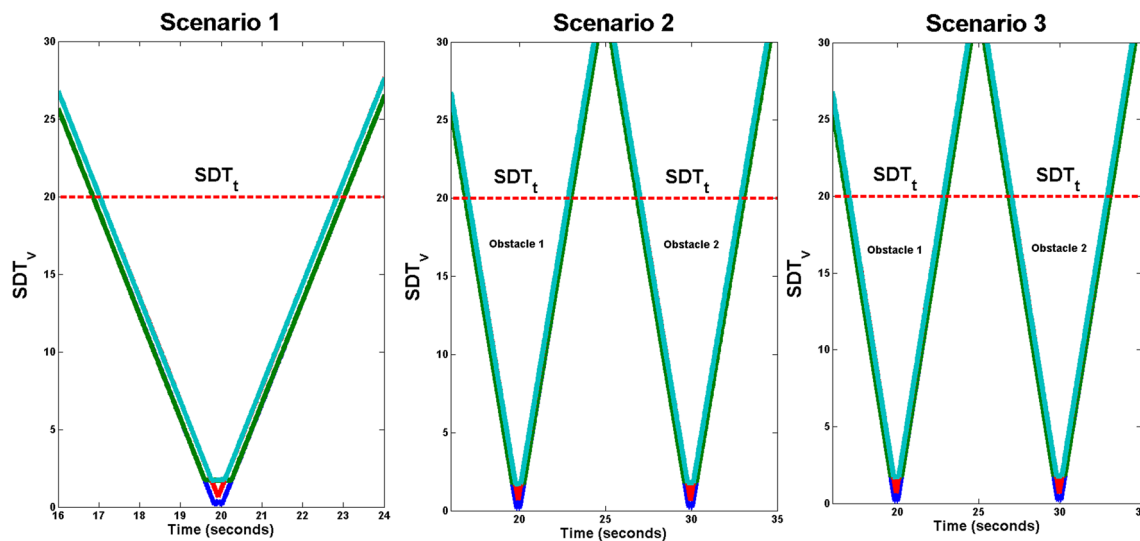
Fig. 15 SDTA formulation for each scenario, where the current value of SDT_v in relation to the threshold, SDT_v is essential in activating the TR actions

4.2.3 Scenario 3: Multiple Static Obstacle, Host Vehicle = 60 km/h

The vehicle moves on a straight road with an initial velocity of 60 km/h. The location of the first frontal vehicle is 330 m in front of the host vehicle initial position, (0, 0). The second obstacle is located at 500 m. The distance from the obstacles to each other is 170 m. As illustrated in Fig. 14c, the host vehicle will avoid the first obstacle before returning to its original trajectory. After the avoidance of the second obstacle, the host vehicle will return to its original lane. The aim of this scenario is to see the reliability of the architecture in assisting the multi-lane change and lane keeping navigation during CA.

4.2.4 Scenario 4: Moving Obstacle = 40 km/h, Host Vehicle = 100 km/h

The vehicle moves on a straight road with an initial velocity of 100 km/h when a frontal moving vehicle is detected. The frontal moving vehicle possesses the same moving axis with the host vehicle and the speed is 40 km/h. The initial distance between the host vehicle with the moving vehicle is 300 m. The collision point between the two vehicles will be at the coordinate (410, 0). The aim of this scenario is to see the reliability of the architecture in avoiding the moving obstacle during high-speed navigation. The scenario is depicted in Fig. 14d.
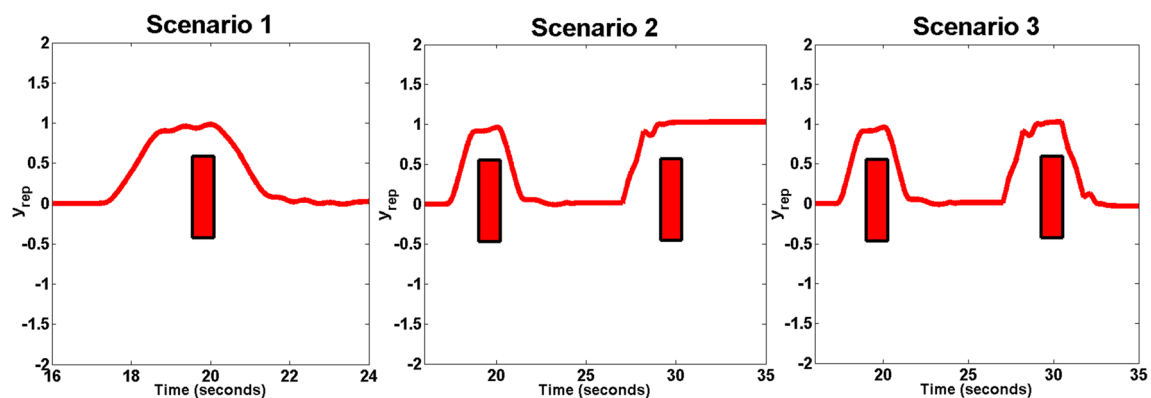

Fig. 16 Reference Replanned Trajectory in relation to the SDTA threshold in Fig. 15
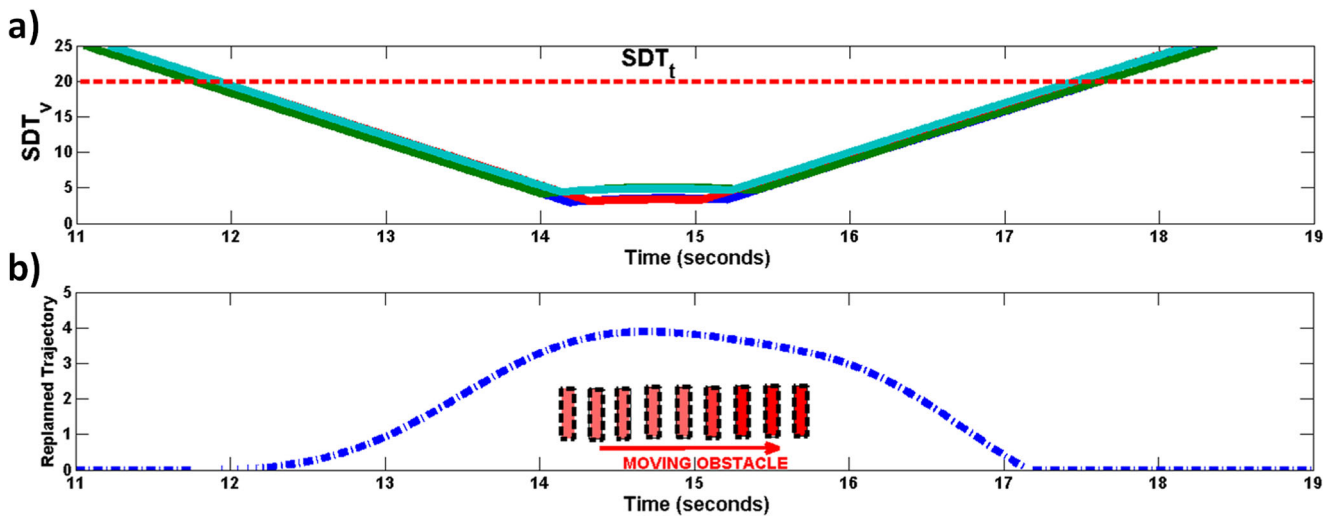
Fig. 17 Trajectory Replanning in relation to the SDTA outputs for the Moving Obstacle scenario (Scenario 4). Red sequence of rectangles represents the moving obstacle

4.3 Threat Assessment Performance

As can be seen in Fig. 15, SDTA provides an online calculation of the distance from each host vehicle's edges to the obstacle's COG. SDT_t represents the threshold which the system must abide by. In Scenario 2 and 3, the SDT_v of the host vehicle's edges to each frontal vehicles are shown.

As in the formulation, the red line depicts the threshold, SDT_t, where the replanning actions in Fig. 16 depends on the threshold values. For dynamic obstacle, the SDTA outputs is shown in Fig. 17a. As can be seen, since the obstacle is moving, the SDT_v possess extended span compared to the one in Scenario 1, 2 and 3. The ability of SDTA to provide the Threat Assessment helps the TR in replanning the trajectory.
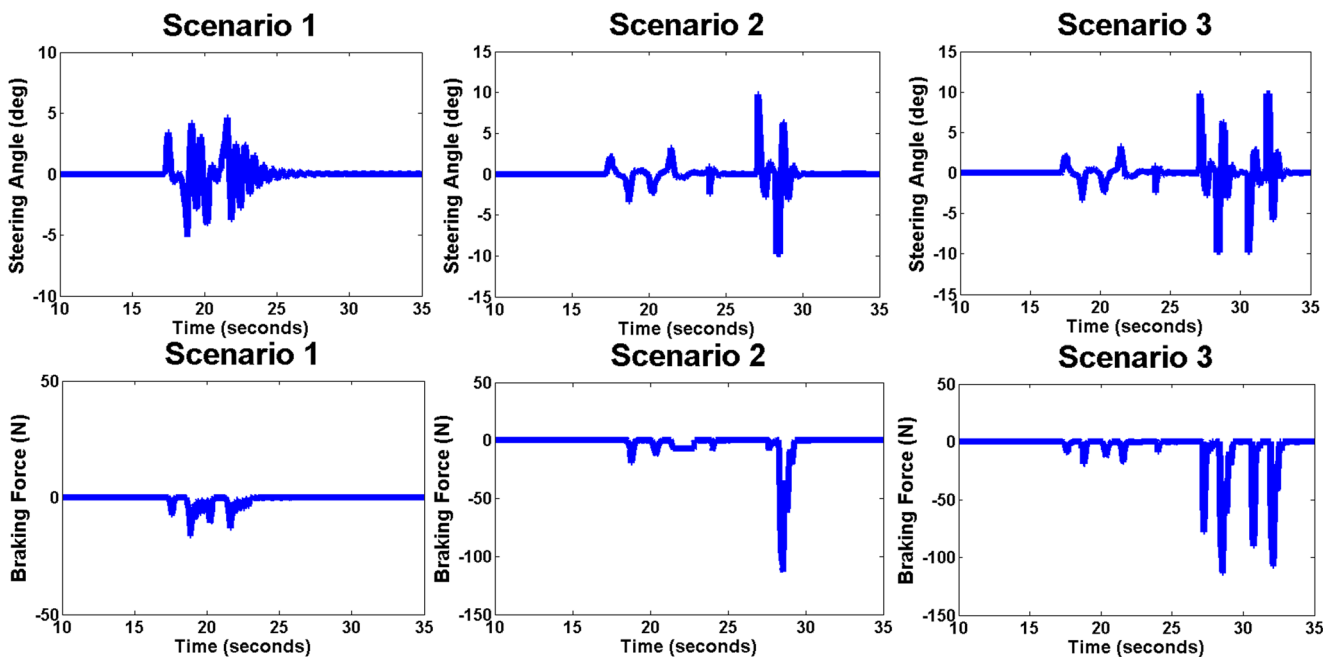

Fig. 18 NMPC Control Actuations (Steering Angle and Braking Torques) for the lane change and lane keeping performance during CA
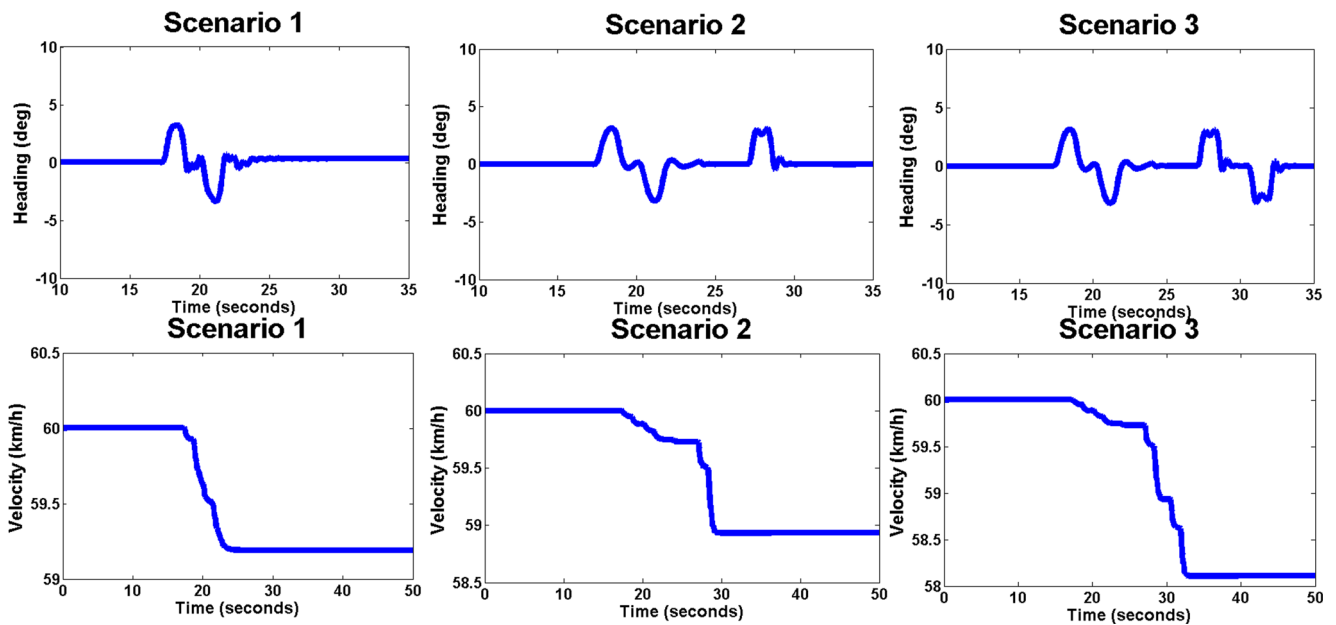
Fig. 19 Vehicle Heading and Velocity while traversing the obstacles

4.4 Trajectory Replanning Performance

Figure 16 illustrates the reference replanned trajectory of the CA system in relation to the SDT_t and SDT_v metrics. The desired heading angle change, θ_{rep} is discrete in the reference path, especially in Scenario 2 and Scenario 3. This is due to the piecewise nature of the replanning actions.

However, the controller will output a vehicle heading that accommodates the vehicle dynamics according to Eq. 1–7. For dynamic obstacle (Fig. 17b), the system is shown to replan the path with larger y_{rep}. This is to allow a feasible CA trajectory during the high-speed maneuver. In addition, a small y_{rep} during the CA navigation for Scenario 4 can result in the collision with the moving vehicle.
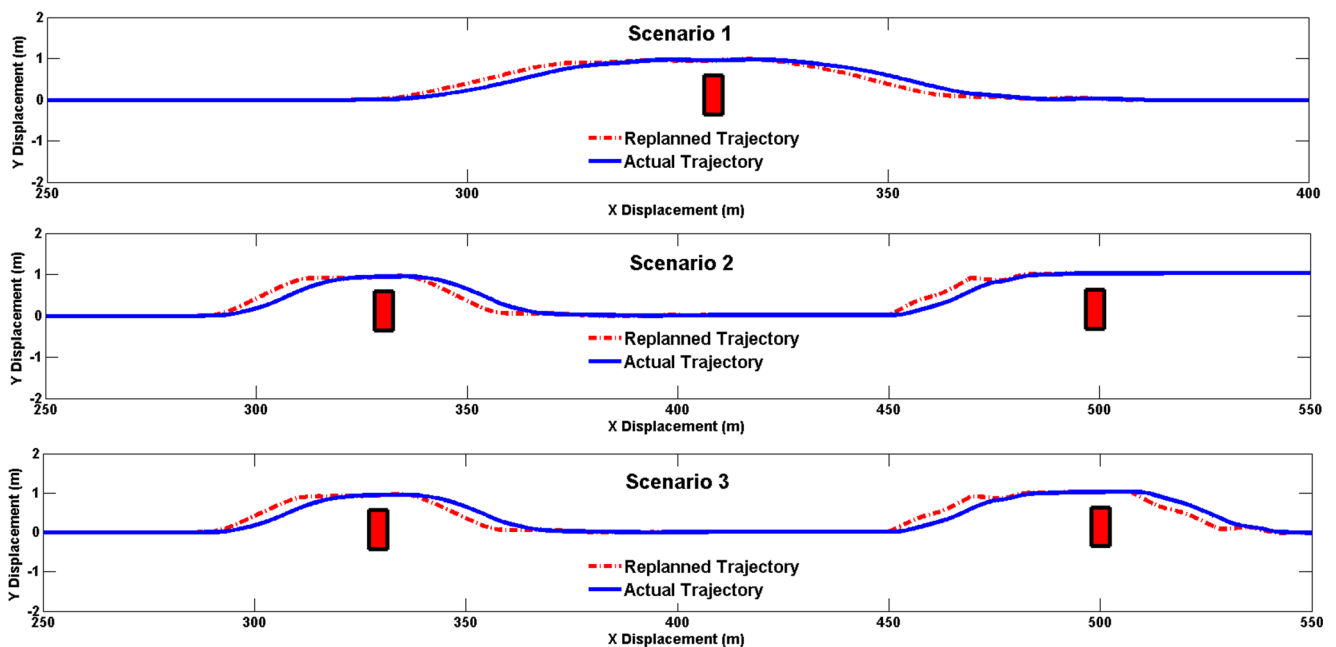

Fig. 20 Collision Avoidance Trajectory of the proposed Architecture for Scenario 1, 2 and 3
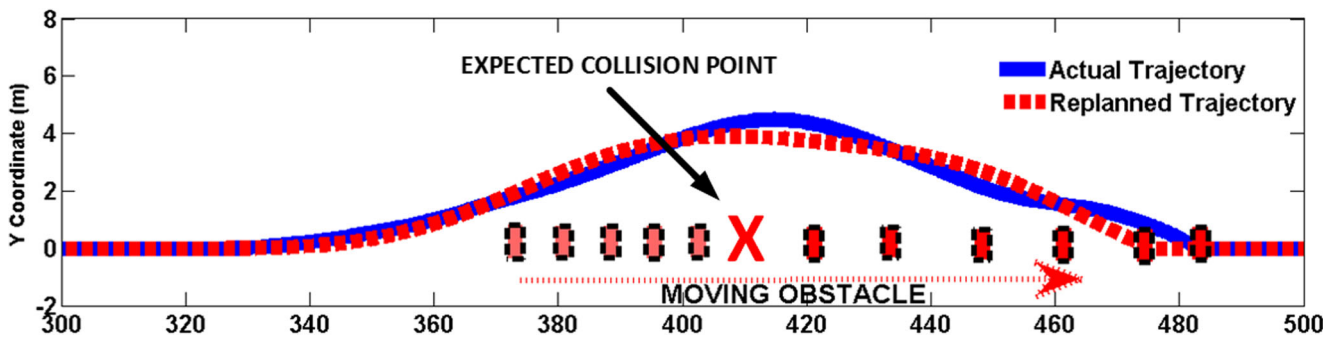
Fig. 21 Avoidance Trajectory for Scenario 4 (Moving Obstacle at High Speed). Red 'X' illustrates the expected collision point between the host vehicle and moving frontal obstacle should there be no CA navigation

4.5 Nonlinear Model Predictive Control Tracking Performance

4.5.1 Lane Keeping and Lane Change Performance

NMPC provides reliable steering angle and braking force actuations in Scenario 1, 2 and 3 (Fig. 18). In Scenario 2 and Scenario 3, due to the short distance between the period of the vehicle returning to the trajectory and avoiding the second obstacle, a larger steering angle and braking force are yielded by NMPC. As can be seen, NMPC helps the vehicle to return to its original trajectory after the avoidance in all of the scenario. For Scenario 3, a prolonged period of steering angle changes are required since the host vehicle are dictated to return to original trajectory, compared to Scenario 2 where the vehicle is not required to return to the original lane after CA maneuver. For braking force, since the vehicle is trying to avoid static obstacles in Scenario 1, 2 and 3 (e.g. parked stranded vehicle), thus, the braking force which is required is not large. In addition, the inclusion of SDTA enables a timely TR activation, and thus allowing a smooth CA navigation which prevents sudden deceleration of the host vehicle.

In Fig. 19, the vehicle heading and velocity of the host vehicle while traversing the obstacles are shown. It is shown that NMPC actuations help the host vehicle to avoid the obstacle and return to its original heading. For velocity, it is shown that the deceleration happened only during the emergence of obstacles since the braking distribution depends on the SDT_v and SDT_t. This help to prevent unnecessary braking actuations.

4.5.2 Avoidance Trajectory with NMPC

From Fig. 20, NMPC is shown to act as the Path Follower to the reference path. The response delay is due to the dynamic of the host vehicle. For Scenario 2 and 3, NMPC is shown to help the host vehicle in traversing the obstacle, ensuring no lane departure in all of the proposed scenarios due to the constraints and state predictions incorporated in its formulation. The braking distributions which are based on the SDTA outputs help to yield feasible CA navigations.

4.5.3 NMPC for Dynamic Obstacle

As for dynamic obstacle with high host vehicle speed, the reference replanned trajectory tracking performance is shown in Fig. 21. Due to the moving obstacle, a larger y_{cur} is evident in the navigation to accommodate the high-speed dynamics of the host vehicle. The vehicle overtakes the red moving frontal vehicle (Fig. 21) while ensuring the safe distance. NMPC guides the host vehicle to follow the reference trajectory and prevent the collision from happening at the expected point (red 'X' in Fig. 21). The moving obstacle is symbolized by the sequence of the red rectangles.

4.5.4 NMPC Trajectory Tracking with Move Blocking Strategy

The results of MB incorporation into NMPC in this work are written in Table 3. The elapsed simulation computational time are considered as comparison metrics of NMPC performance with and without the MB strategy. The

Table 3 Comparison of NMPC computation time with and without Move Blocking Strategy

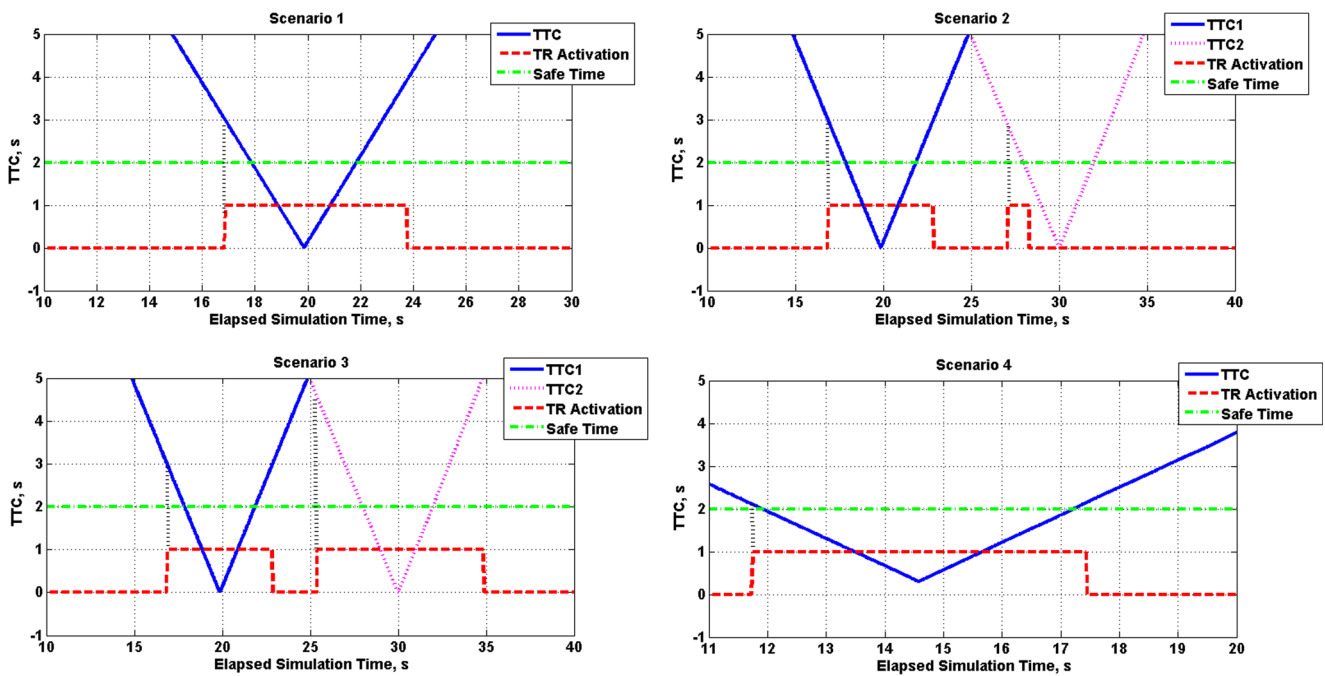| Comparison Metrics	Blocking	Scenario 1	Scenario 2	Scenario 3	Scenario 4
Calculation Time, s	Uniform Blocking	6.624	8.874	9.243	19.263
	Move Blocking	6.159	7.117	8.424	13.883

Fig. 22 The performance of the Trajectory Replanning based on the SDTA compared to the time-to-collision of each scenario. $TTC1$ and $TTC2$ each refers to the TTC for first and second frontal obstacles, for the multiple obstacles scenario. TR is activated when the TR Activation shows the value of $'1'$

computational time for each scenario is measured using the *tic* and *toc* methods of MATLAB [70].

It is evident that NMPC with Move Blocking possesses a lot of advantage, particularly in the Scenario 4 (high nonlinearity), where it reduces a significant amount of the system's computational time (Table 3). From the results, we can conclude that NMPC computational time can be reduced with the assimilation of Move Blocking Strategy while maintaining the tracking performance. With the presence of a better computational device, the real-time implementation of this work will show improved computational time amount.

4.5.5 Time-to-Collision between the Host Vehicle and Frontal Obstacles

The system's reliability in maintaining the safe distance between the host vehicle and obstacle, while subsequently preventing the incidents in a timely manner is evaluated agains an online calculation of the time-to-collision formulation between them (Eq. 32). The results are shown in Fig. 22 for each scenario. In all scenarios, the vehicle manages to avoid the obstacles at least 2 seconds from the expected point collision, which is the x coordinate of the frontal obstacle. This complies with the standard threshold of TTC used in many works such as [71, 72] and [73], which is 2 seconds.

In Table 4, it is shown that the Piecewise Emergency Trajectory Replanner successfully replan the emergency trajectory by maintaining the SDTA and in the same time observing the time-to-collisions. In contrast to the TTC which only considers the safe-time, the inclusion of SDTA into the TR ensures the observation of both TTC and SDTA constraints. Thus, TR is shown to work well as the path replanning strategy and maintaining the safe distance and safe time to the obstacle.

Table 4 The TR performance of the system in relation to the Time-to-Collision. O_1 and O_2 each represents the TTC to the first and second frontal obstacles

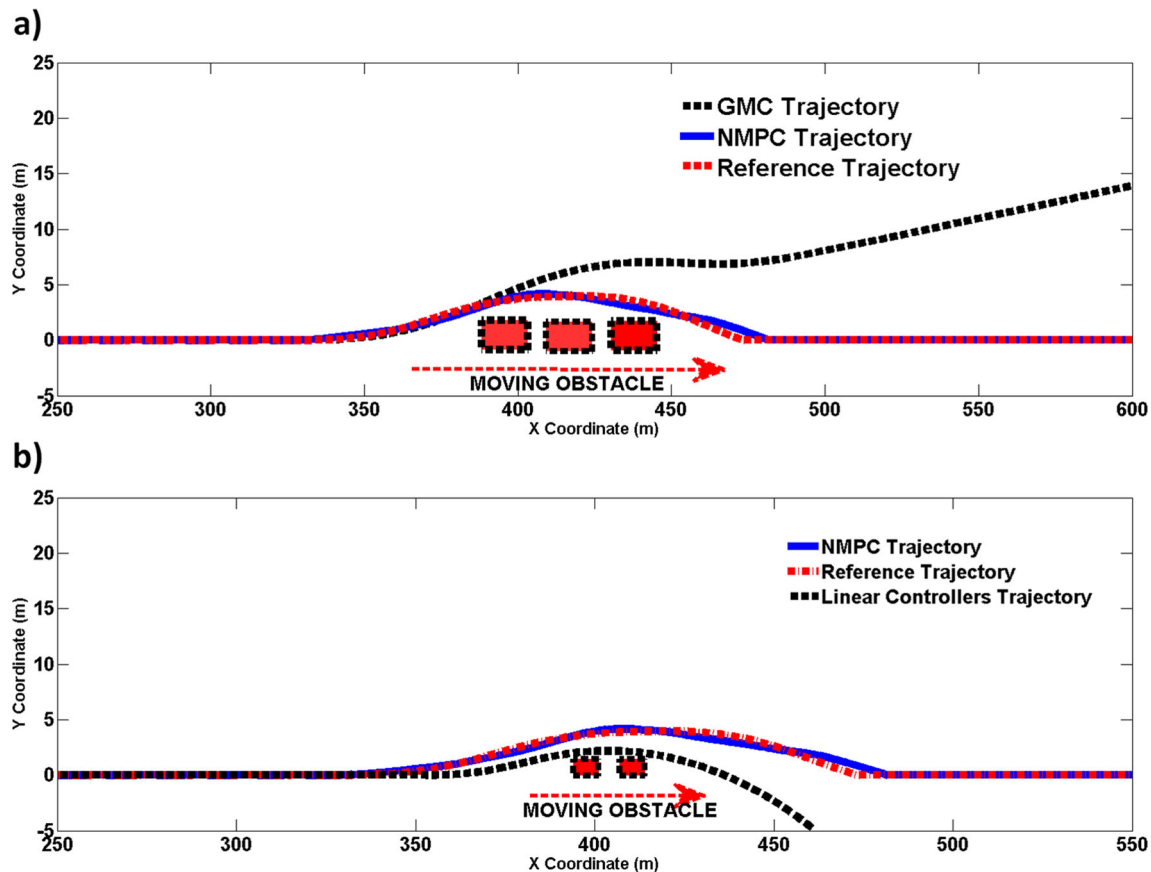| Scenario	Scenario 1	Scenario 2	Scenario 3	Scenario 4
TTC during TR Activation, (s)	2.9661	2.9661 (O_1), 2.8639 (O_2)	2.9661 (O_1), 4.5610 (O_2)	2.0945

Fig. 23 Collision Avoidance Trajectory comparison for the architecture between NMPC and GMC as the PT (**a**), and (**b**) performance comparison between NMPC and Linear Controllers

4.6 Comparisons of the Tracking Controller

4.6.1 Absence of Braking

The comparison between NMPC and GMC as the Path Tracking of the architecture are validated in Scenario 4. From Fig. 23a, it is noticeable that with GMC as the PT, though managed to avoid the obstacle, the host vehicle slid too far away from the original path and crashed into another area. NMPC is shown to perform better since it has the inclusion of braking actuations which complement the steering angle at higher speeds.

4.6.2 Linear Controller vs Nonlinear Controller

In the previous work using the Linear Controllers, the system is validated with controlled host vehicle velocity, 40 km/h [2]. However, since the proposed host vehicle speed in Scenario 4 is higher, as can be seen in Fig. 23b, the linear controllers are not able to handle the vehicle nonlinear dynamics during the navigation. It yields delayed under-

actuated steering controller actuations which subsequently permits lane departure after the avoidance. However, with NMPC, the architecture is able to track the replanned path in the high speed. This is due to its MIMO feature which allows it to handle the combined nonlinearities of the longitudinal and lateral vehicle dynamics. In addition, the inclusion of the vehicle states' vector into NMPC optimization function ensures the reliable tracking performance.

5 Conclusions

This paper proposed a piecewise-kinematic based trajectory replanning strategy for a collision avoidance system. The CA architecture is encompassed of SDTA, TR and PT strategies. It is designed as a solution to the common problems of CA such as unreliable lane change and lane keeping maneuvers in multi-scenario risks, untimely CA navigation, the nonlinearity of high-speed collisions, the absence of multi-actuators CA system as well as side collision with the obstacle edges.

The trajectory replanner is formulated using the SDTA outputs. It is also used for the braking distribution states. The simulations are done to verify the ability of the system to perform lane keeping and lane change CA maneuvers. It is proven that the proposed TR strategy works well in multi-scenario CA. The inclusion of SDTA ensures no side collision between the host vehicle and obstacles, by providing a safe region in its calculations. In addition, this can reduce the incidents of accidents caused by driver inattentiveness. The consideration of the vehicle kinematics into TR formulation ensures a feasible trajectory for the host vehicle. NMPC is then shown to perform well in all scenario as the Path Tracking strategy. Comparisons with benchmark controllers show that the MIMO feature of NMPC as well its nonlinearity nature promise a reliable CA navigation for the host vehicle. The complexity of NMPC which causes high computational time is reduced by assimilating the Move Blocking Strategy.

For future works, a real-time implementation will be done to evaluate the robustness of the proposed design. Furthermore, a more complex multi-objective CA scenario should be used as the case study. For example, CA in crowded urban areas where sudden appearing obstacle might appear at intersections.

The piecewise-kinematic based TR usage is not limited for CA. Consequently, this architecture can be used for other autonomous vehicle usages such as automated parking and mobile robot obstacle avoidance. Further works on the TR consist of improving its usage in a crowded area with unknown dynamic obstacles. A combination of SDTA and Time-to-X algorithms for the risk assessment of the TR, for example, will be advantageous.

For NMPC, it possesses a bright future in the vehicle active safety field. Thus, a more detailed study on its optimization problem should be covered in the future.

As this paper is a simulation-based publication, the authors did not reflect on the sensing aspects of CA. Therefore, a study on this particular area will be beneficial. For example, a combination of this proposed architecture with other systems such as Simultaneous Localization and Mapping (SLAM) and Global Positioning System (GPS) will be helpful in executing the system in real urban areas. In addition, the integration of the system with precise vehicle classifications study will be beneficial to obtain more precise risk assessment in a multi-size highway vehicles collision avoidance (e.g. long trucks etc). This in return will enhance the performance of the TR.

Overall, a piecewise-kinematic based TR strategy for a CA architecture which considers the vehicle dynamic constraints, the safe distance to the obstacle as well as providing integrated controller actions in emergency situations is evaluated in this work. Results show that the TR design is reliable as the non-holonomic path replanning strategy for the vehicle collision avoidance systems in multi-scenario risk occurrence.

References

1. Fleming, W.: Forty-Year Review of Automotive Electronics: A Unique Source of Historical Information on Automotive Electronics. In: IEEE vehicular technology maga-zine. 10th edn., (3), pp. 80–90. IEEE, Piscataway (2015)
2. Raksincharoensak, P., Hasegawa, T., Nagai, M.: Motion Planning and Control of Autonomous Driving Intelligence System Based on Risk Potential Optimization Framework . In: International Journal of Automotive Engineering (7) AVEC14, pp. 53–60 (2016)
3. Ramli, R., Oxley, J., Noor, F.M., Abdullah, N.K., Mahmood, M.S., Tajuddin, A.K., McClure, R.: Fatal injuries among motorcyclists in Klang Valley, Malaysia. J. Forensic Legal Med. **26**, 39–45 (2014). Elsevier
4. Mustafa, M.N.: Overview of current road safety situation in Malaysia (Highway planning Unit, Road Safety Section, Ministry of Works) (2005)
5. Long, A.D., Kloeden, C.N., Hutchinson, P., McLean, J.: Reduction of speed limit from 110 km/h to 100 km/h on certain roads in South Australia: a preliminary evaluation, Centre for Automotive Safety Research (2006)
6. Insurance Institute for Highway Safety (Highway Loss Data Institute), Low- and medium-speed vehicles in IIHS Site retrieved on 18th October 2016 http://iihs.org
7. Insurance Institute for Highway Safety (Highway Loss Data Institute), Speed and Speed Limits in IIHS Site retrieved on 18th October 2016 http://iihs.org
8. Official Portal of Road Transport Department Malaysia, Speed Limits for Malaysian Highway retrieved on 18th October 2016 http://jpj.gov.my
9. Wierwille, W.W., Wreggit, S.S., Kirn, C.L., Ellsworth, L.A., Fairbanks, R.J.: Research on Vehicle-Based Driver Status/Performance Monitoring; Development, Validation, and Refinement of Algorithms for Detection of Driver Drowsiness. Final Report, Virginia Polytechnic Institute and State University, Blacksburg (1994)
10. Kim, S.Y., Kang, J.K., Oh, S.Y., Ryu, Y.W., Kim, K., Park, S.C., Kim, J.: An intelligent and integrated driver assistance system for increased safety and convenience based on all-around sensing. J. Intell. Robot. Syst. **51**(3), 261–287 (2008)
11. Vahidi, A., Eskandarian, A.: Research advances in intelligent collision avoidance and adaptive cruise control. IEEE Trans. Intell. Transp. Syst. **4** (3), 143–153 (2003). (IEEE)
12. National Transportation Safety Board. (2016) NTSB unveils 2016 most wanted list, stresses technology in [Online] Available: http://www.ntsb.gov/NTSBPressRelease
13. Saito, Y., Raksincharoensak, P.: Risk predictive shared deceleration control: Its functionality and effectiveness of an early

intervention support. In: 2016 IEEE intelligent vehicles symposium (IV), pp. 49–54. IEEE, Piscataway (2016)

14. Hayashi, R., Isogai, J., Raksincharoensak, P., Nagai, M.: Autonomous collision avoidance system by combined control of steering and braking using geometrically optimised vehicular trajectory. In: Vehicle system dynamics. 50th edn., (sup1), pp. 151–168. Taylor & Francis, Milton Park (2012)

15. Wongwaiwit, P., Raksincharoensak, P., Michitsuji, Y.: Analysis on Pedestrian and Bicycle Behavior in Unsignalized Intersection Based on Near-Miss Incident Database . In: Proceedings of 20th JSME transportation and logistics conference, pp. 19–22 (2011)

16. Ariff, M.H., Zamzuri, H., Nordin, M.A., Yahya, W.J., Mazlan, S.A., Rahman, M.A.: Optimal control strategy for low speed and high speed four-wheel-active steering vehicle. In: Journal of Mechanical Engineering and Sciences, vol. 8, pp. 1516–1528 (2015). (UMP)

17. Shim, T., Adireddy, G., Yuan, H.: Autonomous vehicle collision avoidance system using path planning and model-predictive-control-based active front steering and wheel torque control. In: Proceedings of the institution of mechanical engineers, part D: journal of automobile engineering, pp. 767–778. Sage Publications, Thousand Oaks (2012)

18. Carvalho, A., Lefévre, S., Schildbach, G., Kong, J., Borrelli, F.: Automated driving: The role of forecasts and uncertainty — A control perspective. In: European Journal of Control, vol. 24, pp. 14–32. Elsevier, Amsterdam (2015)

19. Ahmad, F., Khisbullah, H., Harun, M.H.: Pneumatically actuated active suspension system for reducing vehicle dive and squat. In: Jurnal mekanikal, vol. 28, pp. 85–114 (2009). (UTM)

20. Kutluay, E., Winner, H.: Validation of vehicle dynamics simulation models–a review. Veh. Syst. Dyn. **52**(2), 186–200 (2014)

21. Stallmann, M.J., Els, P.S.: Parameterization and modelling of large off-road tyres for ride analyses: Part 2–Parameterization and validation of tyre models. In: Journal of Terramechanics, vol. 55, pp. 85–94. Elsevier, Amsterdam (2014)

22. Pacejka, H.: Tire and vehicle dynamics. Elsevier, Amsterdam (2005)

23. Turri, V., Carvalho, A., Tseng, H.E., Johansson, K.H., Borrelli, F.: Linear model predictive control for lane keeping and obstacle avoidance on low curvature roads. In: 16th international IEEE conference on intelligent transportation systems (ITSC 2013), pp. 378–383. IEEE, Piscataway (2013)

24. Gray, A., Ali, M., Gao, Y., Hedrick, J.K., Borrelli, F.: Integrated threat assessment and control design for roadway departure avoidance. In: 2012 15th international ieee conference on intelligent transportation systems (ITSC), pp. 1714–1719. IEEE, Piscataway (2012)

25. Gray, A., Ali, M., Gao, Y., Hedrick, J.K., Borrelli, F.: A unified approach to threat assessment and control for automotive active safety. IEEE Trans. Intell. Transp. Syst. **14**(3), 1490–1499 (2013)

26. Hamid, U.Z.A., Zamzuri, H., Raksincharoensak, P., Rahman, M.A.A.: Analysis of Vehicle Collision Avoidance using Model Predictive Control with Threat Assessment. In: 23rd ITS world congress 2016 (Melbourne) (2016). https://doi.org/10.13140/RG.2.2.36369.22889

27. Hamid, U.Z.A., Zamzuri, H., Rahman, M.A., Yahya, W.J.: A Safe-Distance Based Threat Assessment with Geometrical Based Steering Control for Vehicle Collision Avoidance. In: Journal of telecommunication, electronic and computer engineering (JTEC), 8th edn. (2), pp. 53–58 (2016). UTEM

28. Shah, J., Best, M., Benmimoun, A., Ayat, M.L.: Autonomous rear-end collision avoidance using an electric power steering system.

Proceedings of the Institution of Mechanical Engineers, Part D: Journal of Automobile Engineering **229**(12), 1638–1655 (2015). (SAGE)

29. Savino, G., Pierini, M., Baldanzini, N.: Decision logic of an active braking system for powered two wheelers. Proceedings of the Institution of Mechanical Engineers, Part D: Journal of Automobile Engineering **226**(8), 1026–1036 (2012). (SAGE)

30. Chen, Y.-L.: Study on a novel forward collision probability index. Int. J. Veh. Saf. **8** (3), 193–204 (2015). (Inderscience Publishers (IEL))

31. Huang, S.: Autonomous intelligent cruise control with actuator delays. J. Intell. Robot. Syst. **23**(1), 27–43 (1998). Springer

32. Raja, P., Pugazhenthi, S.: Optimal path planning of mobile robots: A review. International Journal of Physical Sciences **7** (9), 1314–1320 (2012). Academic Journals

33. Polden, J., Pan, Z., Larkin, N., van Duin, S.: Adaptive Partial Shortcuts: Path Optimization for Industrial Robotics. In: Journal of Intelligent & Robotic Systems, pp. 1–13, Berlin (2015). Springer

34. Dubins, L.E.: On curves of minimal length with a constraint on average curvature, and with prescribed initial and terminal positions and tangents. Am. J. Math. **79**(3), 497–516 (1957). (JSTOR)

35. Zips, P., Böck, M., Kugi, A.: Optimisation based path planning for car parking in narrow environments. Robot. Auton. Syst. **79**, 1–11 (2016). Elsevier

36. Cheein, F.A., Scaglia, G.: Trajectory tracking controller design for unmanned vehicles: A new methodology. J. Field Rob. **31**(6), 861–887 (2014). Wiley Online Library

37. Zakaria, M.A., Zamzuri, H., Mazlan, S.A.: Dynamic Curvature Steering Control for Autonomous Vehicle: Performance Analysis. IOP Conference Series: Materials Science and Engineering **114**(1), 012149 (2016). IOP Publishing

38. Camacho, E.F., Alba, C.B.: Model predictive control. Springer Science & Business Media, Berlin (2013)

39. Rahmani, B.: Industrial Internet of Things: Design and Stabilization of Nonlinear Automation Systems. In: Journal of Intelligent & Robotic Systems, pp. 1–13. Springer, Berlin (2016)

40. Yakub, F., Mori, Y.: Comparative study of autonomous path-following vehicle control via model predictive control and linear quadratic control. Proceedings of the Institution of Mechanical Engineers, Part D: Journal of automobile engineering **229**(12), 1695–1714 (2015). (Sage Publications)

41. Magni, L., Scattolini, R.: An overview of nonlinear model predictive control. In: Automotive model predictive control, pp. 107–117. Springer, Berlin (2010)

42. Shekhar, R.C., Maciejowski, J.M.: Robust variable horizon MPC with move blocking. Syst. Control Lett. **61**(4), 587–594 (2012). (Elsevier)

43. Lee, J., Nam, Y., Hong, S., Cho, W.: New potential functions with random force algorithms using potential field method. J. Intell. Robot. Syst. **66**(3), 303–319 (2012). (Springer)

44. Al-Sultan, K.S., Aliyu, M.D.: A new potential field-based algorithm for path planning. J. Intell. Robot. Syst. **17**(3), 265–282 (1996). (Springer)

45. Alonso-Mora, J., Naegeli, T., Siegwart, R., Beardsley, P.: Collision avoidance for aerial vehicles in multi-agent scenarios. Auton. Robot. **39**(1), 101–121 (2015). Springer

46. Pacejka, H.B., Bakker, E.: The magic formula tyre model. Veh. Syst. Dyn. **21**(S1), 1–18 (1992). (Taylor & Francis)

47. Buckholtz, K.R.: Use of fuzzy logic in wheel slip assignment–Part I: yaw rate control. In: SAE world congress (2002-01), p. 1221 (2002). (Citeseer)

48. Prestero, T.T.J.: Verification of a six-degree of freedom simulation model for the REMUS autonomous underwater vehicle (PhD Thesis), pp. 1–18. Massachusetts institute of technology, Cambridge (2001)

49. Ali, M., Gsray, A., Gao, Y., Hedrick, J.K., Borrelli, F.: Multi-Objective Collision Avoidance. In: ASME 2013 dynamic systems and control conference, pp. V003T47A004–V003T47A004. American Society of Mechanical Engineers, New York (2013)

50. Lefèvre, S., Vasquez, D., Laugier, C.: A survey on motion prediction and risk assessment for intelligent vehicles. Robomech Journal **1** (1), 1 (2014). (Springer International Publishing)

51. Lee, D., Han, K., Huh, K.: Collision detection system design using a multi-layer laser scanner for collision mitigation. Proceedings of the Institution of Mechanical Engineers, Part D: Journal of automobile engineering **226**(7), 905–914 (2015). (SAGE Publications)

52. Althoff, M., Mergel, A.: Comparison of Markov chain abstraction and Monte Carlo simulation for the safety assessment of autonomous cars. IEEE Trans. Intell. Transp. Syst. **12**(4), 1237–1247 (2011). IEEE

53. Thiel, C., Schmidt, J., Van Zyl, A., Schmid, E.: Cost and well-to-wheel implications of the vehicle fleet CO 2 emission regulation in the European Union. Transp. Res. A Policy Pract. **63**, 25–42 (2014). Elsevier

54. Sfetcu, N.: The Car Show. Lulu Press, ISBN: 9781447876359, Morrisville (2011)

55. Sørbø, E.H.: Vehicle Collision Avoidance System (Thesis). Norwegian University of Science and Technology – Institutt for teknisk kybernetikk, Trondheim (2013)

56. Brimberg, J.: Properties of Distance Functions and Minisum Location Models (Thesis). McMaster University), Hamilton (1989)

57. Khatib, O.: Real-time obstacle avoidance for manipulators and mobile robots. In: The International Journal of Robotics Research. 5th edn., (1), pp. 90–98. SAGE, Newcastle upon Tyne (1986)

58. Schmitt, S., Le Bars, F., Jaulin, L., Latzel, T.: Obstacle avoidance for an autonomous marine Robot—A vector field approach. In: Quantitative monitoring of the underwater environment, pp. 119–131. Elsevier, Amsterdam (2016)

59. Vilca, J.M., Adouane, L., Mezouar, Y.: Optimal Multi-Criteria Waypoint Selection for Autonomous Vehicle Navigation in Structured Environment. J. Intell. Robot. Syst. **82**(2), 301–324 (2016). Springer

60. Vehicle Stopping Distance and Time in National Association of City Transportation Officials sites, retrieved on 24th April 2017 http://nacto.org/

61. Attia, R., Orjuela, R., Basset, M.: Combined longitudinal and lateral control for automated vehicle guidance. Veh. Syst. Dyn. **52**(2), 261–279 (2014). (Taylor & Francis)

62. Longo, S., Kerrigan, E.C., Ling, K.V., Constantinides, G.A.: Parallel move blocking model predictive control. In: 2011 50th IEEE conference on decision and control and european control conference, pp. 1239–1244. IEEE, Piscataway (2011)

63. Norén, C.: Path Planning for Autonomous Heavy Duty Vehicles Using Nonlinear Model Predictive Control. PhD Thesis, Linköpings Universitet (2013)

64. Cagienard, R., Grieder, P., Kerrigan, E.C., Morari, M.: Move blocking strategies in receding horizon control. J. Process Control **17**(6), 563–570 (2007). (Elsevier)

65. Mikuláš, O.: A framework for nonlinear model predictive control. 2016 Thesis Czech technical university in Prague (2016)

66. Zakaria, M.A., Zamzuri, H., Mamat, R., Mazlan, S.A.: A path tracking algorithm using future prediction control with spike detection for an autonomous vehicle robot. In: International Journal of Advanced Robotic Systems, vol. 10. InTech, Rijeka (2013)

67. Garriga, J.L., Soroush, M.: Model predictive control tuning methods: A review. Ind. Eng. Chem. Res. **49**(8), 3505–3515 (2010). (ACS Publications)

68. Joe, H., Xu, J.J.: The estimation method of inference functions for margins for multivariate models. University of British Columbia, Vancouver (1996)

69. Rybus, T., Seweryn, K., Sasiadek, J.Z.: Control system for free-floating space manipulator based on nonlinear model predictive control (NMPC). In: Journal of Intelligent & Robotic Systems, pp. 1–19. Springer, Berlin (2016)

70. Knapp-Cordes, M., McKeeman, B.: Improvements to tic and toc functions for measuring absolute elapsed time performance in MATLAB. In: MATLAB Digest (doc. 91934v00), Tech. Rep (2011)

71. Dagan, E., Mano, O., Stein, G.P., Shashua, A.: Forward collision warning with a single camera. In: Intelligent vehicles symposium, pp. 37–42. IEEE, Piscataway (2004)

72. Käfer, E., Hermes, C., Wöhler, C., Ritter, H., Kummert, F.: Recognition of situation classes at road intersections. In: 2010 IEEE international conference on robotics and automation (ICRA), pp. 3960–3965. IEEE, Piscataway (2010)

73. Wakasugi, T.: A study on warning timing for lane change decision aid systems based on driver's lane change maneuver. In: Proceedings 19th international technical conference on the enhanced safety of vehicles, paper, pp. 05–0290 (2005)

Umar Zakir Abdul Hamid Malaysian based Postgraduate Researcher, previously doing his Ph.D. at Universiti Teknologi Malaysia in the Vehicle Collision Avoidance field. He received his Master of Engineering in the Control field from Moscow Aviation Institute, Russia. During the PhD study period, Umar Zakir has been in Tokyo doing his Ph.D. Attachment at Pongsathorn Laboratory, under the supervision of Associate Prof. Pongsathorn Raksincharoensak. His Ph.D. project includes close collaboration with PROTON Holdings Berhad, Malaysian carmaker.

Mohd Hatta Mohammed Ariff is a senior lecturer in Malaysia-Japan International Institute of Technology, Universiti Teknologi Malaysia, Kuala Lumpur. He received his Ph.D. from Universiti Teknologi Malaysia. He is currently with the Vehicle System Engineering iKohza research lab, where his main research interests are Vehicle Dynamics.

Hairi Zamzuri is an academic staff in Universiti Teknologi Malaysia (UTM). He received his Ph.D. in the field of Artificial Intelligence and Control Design from Loughborough University. His research interest is in the area of integrated vehicle dynamic control and active safety technology for ground vehicles. He is currently heading a research lab under collaboration between UTM and Perusahaan Otomobil Nasional Sdn Bhd (Proton), a Malaysian National car manufacturer. Among the success of the lab under his leadership is developing a semi-autonomous vehicle, MyCEV as a platform for a continuous research in the vehicle active safety field.

Yuichi Saito is an Assistant Professor (Researcher) based in Tokyo University of Agriculture & Technology (Pongsathorn Laboratory), Japan. His research interests include Accident Analysis, Road Safety and Transport Modeling.

Muhammad Aizzat Zakaria a senior lecturer in Universiti Malaysia Pahang, Dr Muhammad Aizzat obtained his Ph.D. from Universiti Teknologi Malaysia. His main research interests are in the field of Path Tracking for Autonomous Vehicles and Mobile Robotics. Previously, he did his Ph.D. with the Vehicle System Engineering iKohza research group in Universiti Teknologi Malaysia, Kuala Lumpur.

Mohd Azizi Abdul Rahman earned his Doctorate Degree in Functional Control System from Shibaura Institute of Technology. Previously, he spent several years in the Liverpool University, the United Kingdom for his undergraduate years. A Senior Lecturer in Universiti Teknologi Malaysia (UTM), he is a registered member of IEEE and has won several international awards in the field of robotics and control system. His current research interests include the Vehicle Dynamics and System Level Modelling field.

Pongsathorn Raksincharoensak currently working as an Associate Professor at Smart Mobility Research Center, Tokyo University of Agriculture and Technology (TUAT), Dr. Pongsathorn Raksincharoensak is a well-known academician in the area of Intelligent Transportation Systems. He completed his Doctorate study at the Department of Mechanical Systems Engineering, TUAT and until now has been studying the field of Vehicle Dynamics for more than a decade. Pongsathorn Laboratory in TUAT was established in 2006 as one of the Strategic Division of Young Researchers, funded by Japan Science and Technology Agency (JST) to focus on research regarding automotive dynamics and vehicle active safety.